Journal of Applied Phycology (2026) 38:883–907
https://doi.org/10.1007/s10811-025-03779-4

RESEARCH

Biorefinery of red macroalgae from Madeira archipelago for value-added products

Nuno Nunes[1,2] · **Ana C. Vieira**[1,3,4] · **Kilian Odenthal**[1] · **Miguel Â. A. Pinheiro de Carvalho**[1,2,5]

Received: 3 October 2025 / Revised: 20 November 2025 / Accepted: 29 December 2025 / Published online: 19 January 2026

Abstract

Red macroalgae represent an underexplored yet promising resource due to their rich composition in proteins, pigments, and bioactive compounds with potential uses in nutraceutical, pharmaceutical, and agricultural industries. However, despite their abundance in coastal regions many species remain neglected and the development of efficient extraction and valorisation methods is still limited. This work assesses the optimization of protein and phycoerythrin extraction from three abundant red macroalgae species, *Grateloupia lanceola*, *Asparagopsis taxiformis*, and *Nemalion elminthoides* collected in Madeira island. Its major objective was to study a new biorefinery concept. The response surface methodology (RSM) results indicate that *G. lanceola*, harvested from offshore fish farms, exhibits the highest concentrations of both protein (2967 mg L^{-1}) and phycoerythrin (212 mg L^{-1}) when subjected to specific extraction parameters such as higher biomass weight (400 g) and increased number of cycles (18) using the Solid–Liquid Extraction system. In contrast, *A. taxiformis* and *N. elminthoides* demonstrated varied extraction patterns, with *A. taxiformis* producing substantial protein concentrations (328 mg L^{-1}) but lower phycoerythrin yields (11 mg L^{-1}). Sequential biorefinery methods were also employed to obtain bioactive compounds, and polysaccharides extracts. *G. lanceola* yields the highest concentration of soluble proteins (6.25 ± 0.59 g $(100\ g)^{-1}$ dw) and polysaccharides (11.13 ± 4.85 g $(100\ g)^{-1}$ dw), while *N. elminthoides* showed superior bioactive extract concentration (11.81 ± 0.31 g $(100\ g)^{-1}$ dw). The phenolic content in bioactive extracts has also been assessed using the Folin Ciocalteu method, finding a significant variation in total phenolic content among the species (1.38 ± 0.22 and 5.16 ± 0.06 mg GAE g^{-1} dw). The chromatographic analysis, formed by a Waters HPLC system and a photodiode array detector (Waters 2996) allowed to detect phenolic compounds within the bioactive extract, which include protocatechuic acid, hydroxybenzoic acid, epicatechin, p-coumaric acid and ferulic acid. Furthermore, the agronomic potential of the biorefinery residues was explored, revealing high nitrogen and phosphorus contents in liquid and solid residues, suggesting their potential to be used as biofertilizers. These findings contribute to the development of sustainable extraction processes for bioactive compounds from red macroalgae, enhancing the efficiency of biorefinery strategies and promoting the marine biomass valorization.

Keywords Cascade biorefinery · Biochemical analysis · Macroalgae profile · Agronomic application

✉ Nuno Nunes
nuno.nunes@staff.uma.pt

[1] ISOPlexis Centre for Sustainable Agriculture and Food Technology, University of Madeira, Campus da Penteada, 9020-105 Funchal, Portugal

[2] Centre for the Research and Technology of Agroenvironmental and Biological Sciences, CITAB, Inov4Agro, Universidade de Trás-Os-Montes E Alto Douro, UTAD, Quinta de Prados, 5000-801 Vila Real, Portugal

[3] Faculty of Exact Sciences and Engineering, University of Madeira, Campus da Penteada, 9020-105 Funchal, Portugal

[4] Institute for Nanostructures, Nanomodelling E Nanofabrication, University of Aveiro, 3810-193 Aveiro, Portugal

[5] Faculty of Life Sciences, University of Madeira, Campus da Penteada, 9020-105 Funchal, Portugal

Introduction

Macroalgae represents a promising source of diverse bioactive compounds with applications in food, pharmaceuticals, and nutraceuticals (Guo et al. 2022; Carpena et al. 2023). Because they grow in marine environments, macroalgae do not use arable land or rely heavily on fresh water in the way terrestrial crops do. Large-scale cultivation has been practiced sustainably in many Asian regions, particularly through low-impact, community-based systems. The expansion of high-intensity farming models in new environments may introduce ecological concerns. These can raise serious issues since commercial intensive cultivation may compete with other photosynthetic organisms for light and nutrients, alter trophic interactions, and require substantial inputs of water or energy in post-harvest processing (Campbell et al. 2019). Optimal farm designs and careful life-cycle assessment are needed to ensure that macroalgae production provides real sustainability benefits (Bo et al. 2024). Macroalgae are divided into brown (Class Phaeophyceae), red (Phylum Rhodophyta) and green (Phylum Chlorophyta), and are important sources of bioactive compounds with antioxidant activity (Luan et al. 2024), synthesized to protect the organism from the sea harsh conditions, having a direct influence on its composition (Abraham et al. 2019; Elizondo Sada et al. 2024). The combination of light, salinity, oxygen, low or high temperatures and pressure, and low concentration of nutrients, which increase oxidative stress, induce macroalgae to develop mechanisms for quick acclimation, improving their resilience by producing secondary metabolites, including phycobiliproteins, thus enabling protection from oxidative stress (Ruiz-Medina et al. 2022; Zepeda et al 2025). Given this biochemical diversity, an important strategy is to develop methodologies that could extract and purify more than one compound from this biomass, increasing the efficiency of the process to reach an economic feasibility and reduce waste (del Río et al. 2021). Integrating macroalgae into a biorefinery concept is a path towards a low carbon economy, increasing long term sustainability (Zhu et al. 2023). The biorefinery strategies were envisioned by a well-established and extremely lucrative industry, the fossil fuel refineries (Conteratto et al. 2021). But with the increasing concern about climate change, adjustments should be introduced in the current paradigm. Currently, two strategies are used in biorefinery implementation. First level biorefineries are based on multiple compound extraction near or in their native form, producing high value compounds for food, nutraceutical and pharmaceutical purposes. Second level biorefineries convert whole biomass into the final products, being more appropriate to energy related commodities (Baghel 2023). Several publications have already described the challenges of biorefining high value products and energy related commodities from macroalgae (Abraham et al. 2019; Nunes et al. 2019; Baghel et al. 2020; Nazemi et al. 2021; Zhu et al. 2023; Elizondo Sada et al. 2024; Luan et al. 2024; Martins et al. 2024). A small number of research papers have targeted exclusively the products extracted and purified from red macroalgae due to their unique composition (Nunes et al. 2018; Gomes-Dias et al. 2024; Tenci et al. 2024; Pacheco et al. 2025). Phycobiliproteins, a family of light-harvesting macromolecules present in red macroalgae and a high value product, are a complex structure of pigments and proteins, vital in the photosynthetic apparatus (Apt et al. 1995; Sudhakar et al. 2015). These exhibit a strong absorbance and fluorescence, and especially due to their antioxidant (Romay et al. 1998), anti-inflammatory (Shih et al. 2009) and anti-aging (Feng et al. 2022) activity, can be widely used in foods, cosmetics and pharmaceuticals (Sonani 2016). To efficiently extract phycobiliproteins, protocols must be optimized due to their location on the thylakoid membrane and stroma in the chloroplast (Beattie et al. 2018). Due to their high extraction costs, several strategies are being developed, increasing economic feasibility (Pereira et al. 2020).

Red macroalgae are known as a source of polysaccharides comprising cellulose, agar and carrageenan (Baghel 2023). These macromolecular polymers are abundant in macroalga cell walls, accounting for up to 80% of dry weight, assembled with glucose and galactose monosaccharide units, linked by glycosidic bonds (Mettwally et al. 2022). Polysaccharides have a great applicability in the food industry as a texturizing agent, used in all sorts of products as an emulsifier, thickener, gelling agent and stabilizer (Chevenier et al. 2023). Extracted and purified sulfated polysaccharides have several biological activities namely antibacterial (Jasem et al. 2023), antioxidant (Tesvichian et al. 2024), immunomodulatory (Qin et al. 2022), anti-inflammatory (Jayawardhana et al. 2023), antidiabetic (Pillay et al. 2024), anticoagulant (Wijesinghe et al. 2011) and anticancer (Trung et al. 2024). Carrageenans are of great interest for these industries and extracted from many genera such as *Chondrus*, *Hypnea*, *Gigartina*, *Kappaphycus* and *Eucheuma*, the last two being the most used (Shafie et al. 2022).

Considering a biorefinery strategy, in which several products are sequentially extracted, non-valorized byproducts are expected, and these can be assessed and quantified, envisioning their use in agriculture. Nowadays it is widely investigated, considering that macroalgae, algal extracts and residues have the potential to act as biostimulants, enhancing nutrient efficiency, tolerance to abiotic stress and improving overall crop quality (Mughunth et al. 2024). Efforts have been made to evaluate the efficacy of macroalgal compost

and biochar to ameliorate soil and remove pollutants. Macroalga biomass originates from several environments including seashores, coastal regions, lakes, ponds, rivers and municipal wastewaters which biochar production can be achieved through several thermochemical methods, such as torrefaction, pyrolysis, gasification, and hydrothermal conversion (Dang et al. 2023). For instance, the green alga *Oedogonium intermedium*, cultivated in municipal wastewater, was shown to efficiently recover nitrogen and phosphorus. The harvested biomass was subsequently converted into compost and biochar, which demonstrated potential as soil amendment and at the same time, reducing the anthropogenic footprint (Cole et al. 2017).

Composting macroalgae has several beneficial attributes including a significant weight reduction due to loss of moisture content, which in *Sargassum fluitans* and *S. natans* can lead to a 90% weight loss (Abdool-Ghany et al. 2023). Also, stimulates rapid carbon biodegradability and although nitrogen levels are relatively modest (1 to 2% dry weight), phosphorus, potassium, and trace elements such as Fe, Zn, and Mg are conserved at agronomically relevant levels (Madejón et al. 2022; Abdool-Ghany et al. 2023; Dang et al. 2023).

The hypothesis developed in this work was that locally abundant red macroalgae from the Madeira Archipelago could provide a sustainable biomass resource for the development of a biorefinery strategy. This study focuses on macroalgae species naturally occurring in appreciable amounts along the coasts of Madeira Island and evaluates their potential to generate multiple value-added products within a circular economy framework, while also assessing the resulting non-valorized byproducts as potential biofertilizers for agricultural soils.

Material and methods

Macroalgae from Madeira archipelago

Specimens of *Asparagopsis taxiformis* (Delile) Trevisan (coordinates 32.647155, −16.824185), *Grateloupia lanceola* (J.Agardh) J.Agardh (coordinates 32.659932, −17.053886) and *Nemalion elminthoides* (Velley) Batters (coordinates 32.734273, −16.745741) were collected. Approximately 5 kg fresh weight were harvested for each species at a maximum 10 m depth in the Madeira archipelago. Specimens of *A. taxiformis* and *N. elminthoides* were collected in the subtidal zone, whereas *G. lanceola* was collected in *Sparus aurata* fish cages, positioned greater than 600 m offshore. Collected at the end of spring, samples were transported in seawater to the laboratory, gently rinsed with filtered distilled freshwater to remove surface salts and epiphytes, vacuum-packed, and stored at –35 °C until use. Although brief rinsing may lead to some loss of water-soluble compounds (Wirenfeldt et al. 2022), it was considered necessary to ensure sample cleanliness and standardization, and similar protocols are widely reported in seaweed bioprocessing studies (Cotas et al. 2021).

Optimization of protein and phycoerythrin extraction

To optimize extraction, a 3^2 full factorial design was conducted, including the macroalgae fresh weight factor with three levels (100, 200 and 400 g), placed in a 100 µm nylon filter bag (PM0100). The second factor was the number of cycles used in a semiautomatic pressurized liquid extractor (Timatic Micro-DP-LT.0.5–1–2, Technolab, Italy) also with three levels (6, 12 and 18 cycles). The equipment was set at a constant pressure and static phase during the experiments. Program was set as follows: solvent capacity 0.5 L (phosphate buffer 0.1 M pH 6.8), compression time 3 min, decompression time 6 min, minimum pressure 6 bar, compression pressure 8.5 bar at ± 4 ºC. There were a total of 9 experiments for each macroalga, and process time varied with the number of cycles: 6 cycles run for 54 min, 12 cycles for 108 min and 18 cycles for 162 min. At the end of each run, extracts were centrifuged at 15 000 × *g* for 10 min at 4 ºC. The supernatant was named "crude extract" and assessed for protein and phycoerythrin (PE) content, to determine the best set for higher yield.

Biorefinery methodology

The method selected (Fig. 1) includes an initial protein extraction, using a phosphate buffer (0.1 M, pH 6.8) at 4 ºC temperature, with the Timatic semiautomatic extractor set at a constant pressure, 8.5 bar, and static phase using one of the 3 volume vessels, 0.5-L, 1-L or 2-L to assess the scaling up. The optimal biomass to solvent ratio found and used in this work was 110 g fresh weight per litter of solvent, extracting for 18 cycles with the Timatic extractor. The liquid extract was centrifuged at 15,000 × *g* at 4 ºC and subjected to 2 steps of protein precipitation, 30 and 90%, using solid ammonium sulphate. The addition was performed slowly at 4 ºC under low agitation and, in each step, the mixture was left overnight for complete dissolution. Afterwards, the liquid was centrifuged (30 and subsequent 90% ammonium sulphate) at 15,000 × *g* for 15 min at 4 ºC, for protein precipitation. The solid phase was recovered, homogenized with phosphate buffer (0.1 M, pH 6.8) and dialyzed against the same buffer at 4 ºC, for 24 h to remove the ammonium sulphate salt. This protein extract was reserved and assessed later. The 1st solid residue was carefully rinsed with distilled water to remove the phosphate buffer salts and subjected to a second extraction, using 96% ethanol, again using the Timatic extractor, for 18 cycles at 22ºC. This ethanolic extract was afterwards

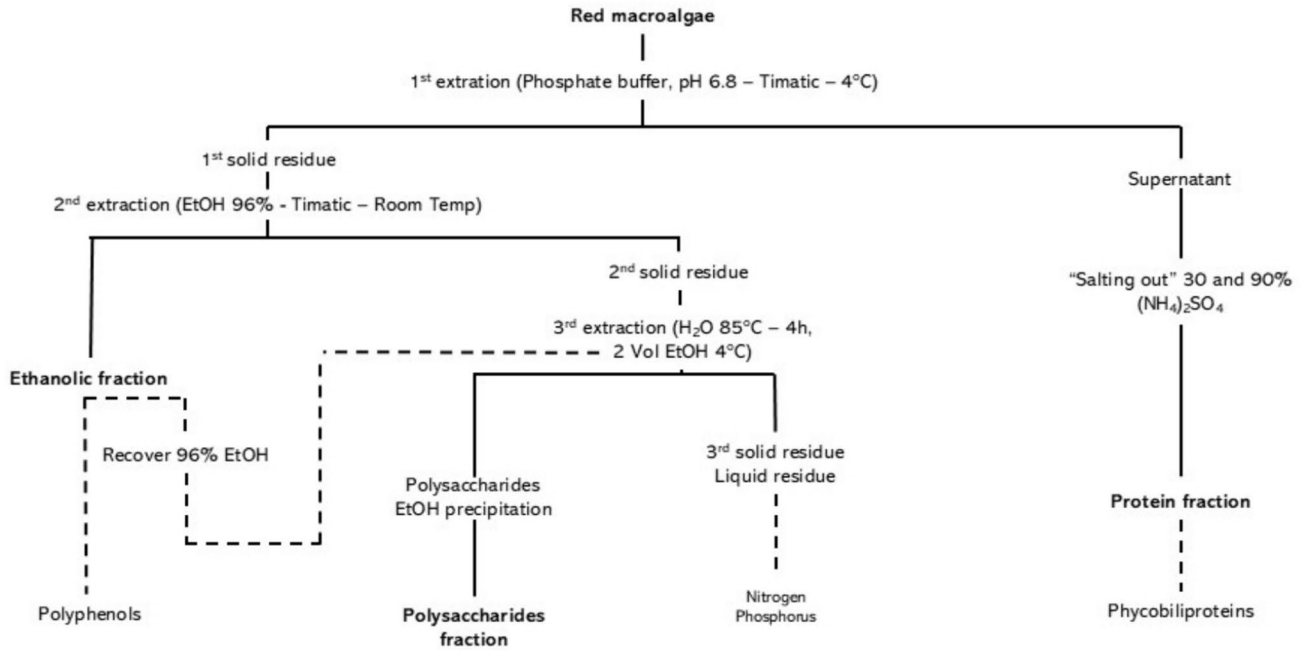

Fig. 1 Biorefinery strategy diagram

passed through an 8 µm cellulose Whatman filter and concentrated using a rotary evaporator, to recover the ethanol and accelerate the drying process, which was conducted in an oven (Memmert UF 260, Germany) at 40 ºC. This is the 2nd extract obtained from the biomass and named in this work as a bioactive extract. After, the 2nd solid residue was dried, also at 40 ºC, and used for the extraction of polysaccharides. The 2nd solid residue was subjected to a water extraction, at 85 ºC, for 4 h. The water extract was then centrifuged at 7200 × *g* for 10 min at 21 ºC and passed through an 8 µm cellulose Whatman filter. After, 2 volumes of 96% ethanol at 4 ºC were added to 1 volume of the water extract and the polysaccharides were separated by centrifugation (7200 × *g* for 10 min at 21 ºC), which remained at the bottom of the container. With this process resulted a liquid residue, composed of ethanol and water and a solid residue. Both were dried at 40 ºC until complete dryness.

Protein and phycoerythrin content

The soluble protein concentration was assessed following the Lowry method (Waterborg 2002). Briefly, the sample was solubilized with distilled water and a mixture of 2% sodium carbonate in 0.1 N sodium hydroxide with 1% potassium sodium tartrate and 0.5% copper sulphate was added in a 50 to 1 proportion. The mixture was incubated for 30 min and then Folin Ciocalteu reagent (diluted in an equal proportion with distilled water) was added. After, the absorbance was read at 750 nm. A standard calibration curve was performed using Bovine Serum Albumine fraction V (BSA). All measurements were performed in triplicate. The results were calculated and expressed as mg L^{-1}. The calibration equation for protein (2.5–480 µg mL^{-1}) was $Y = 0.0023x + 0.0421$ ($R^2 = 0.979$).

The 1st phosphate buffer extracts named as "crude extracts", the protein precipitation fractions, performed with 30 and 90% ammonium sulphate and the supernatant were all assessed for their protein and PE concentration. The resulting precipitated protein, using the 30 and 90% ammonium sulphate, were further solubilized with 15 mL of the same buffer. The PE, Eq. 3, was quantified with a Shimadzu PC-2401 spectrophotometer (Kyoto, Japan), according to the Eqs. 1 (Phycocyanin, PC) and 2 (Allophycocyanin, APC) described below (Bennet and Bogorad 1978; Sudhakar et al. 2015). All measurements were performed in triplicate. The results were calculated and expressed as mg mL^{-1}.

$$PC\left(mg\ mL^{-1}\right) = \frac{\left[A_{615} - 0.474 * A_{652}\right]}{5.34} \quad (1)$$

$$APC\left(mg\ mL^{-1}\right) = \frac{\left[A_{652} - 0.208 * A_{615}\right]}{5.09} \quad (2)$$

$$PE\left(mg\ mL^{-1}\right) = \frac{\left[A_{562} - 2.41 * PC - 0.849 * APC\right]}{9.62} \quad (3)$$

As an additional measure of purity, the PE fluorescence was measured using special 96 well plates (Thermo Scientific Nunc F96 MicroWell Black Polystyrene Plate), using excitation and emission wavelengths of 550 and 576 nm (Varioskan Lux, Thermo Scientific, Singapore), respectively. The results are presented as Relative Fluorescence Units (RFU).

Fast Protein Liquid Chromatography (FPLC)

The most concentrated PE samples, one from each macroalga, were selected to be injected in a FPLC equipment (AKTA prime plus, Sweden) using a Size Exclusion Chromatography HiPrep 16/60 Sephacryl S-200 HR column with a bed volume of 120 mL. The running conditions consisted of a flow rate of 0.8 mL min^{-1}, a 5 mL sample loop, phosphate buffer as the eluent, and absorbance wavelength was set to 280 nm. The FPLC experiment was run inside a PHCBI MPR-1412 chamber (Japan), at 4 ºC. Protocols of ÄKTA Prime Plus equipment and Sephacryl columns from GE HealthCare were followed.

Total phenolic content (TPC)

TPC was assessed using Folin Ciocalteu method (Chew et al. 2008), mixing 1.5 mL Folin Ciocalteu's phenol reagent with 1.2 mL Na_2CO_3 (7.5% w/v) and 0.3 mL sample extract. The mixture was incubated in the dark for 30 min and the absorbance was measured at 765 nm. The results are presented in mg of gallic acid equivalents (GAE) per gram in dry weight (dw) of extract (mg GAE g^{-1} dw). The calibration equation for GAE (25—125 mg L^{-1}) was $Y = 0.0083x - 0.047$ ($R^2 = 0.9854$).

Bioactive extracts analytical assessment

All the bioactive algal extracts were screened for the presence of phenolic compounds, including gallic acid, protocatechuic acid, hydroxybenzoic acid, catechin, chlorogenic acid, caffeic acid, vanillic acid, epicatechin, epigallocatechin gallate, syringic acid, vanillin, p-coumaric acid, syringaldehyde, ferulic acid, rutin, sinapic acid, myricetin, resveratrol, quercetin and kaempferol. For a precise quantification of phenolic compounds in bioactive extracts, samples were injected into a High-Pressure Liquid Chromatograph (HPLC). For sample preparation, algae extracts were directly filtered using polypropylene syringe filters (0.20 µm) from BGB (China) and 20 µL of each sample were injected. Samples were spiked with a standard solution for peak identification. When not promptly analyzed, extracts were kept at 4 °C, to avoid sample degradation. For calibration, individual phenolic compounds solutions (2 g L^{-1}) were prepared in ethanol (0.1% formic acid) and a stock solution (50 mg L^{-1}) was prepared by dissolving all the standard solutions in water (0.1% formic acid). From this solution, at least 5 diluted solutions were prepared in triplicate. Phenolic compounds were determined in an HPLC system using a Waters (USA) liquid chromatograph connected to Empower Pro Software and equipped with an auto-injector (Waters 2695, separation module) and a photodiode array detector (Waters 2996). Chromatographic analyses were performed using a reversed-phase C18 column (Atlantis T3, 3 mm × 250 mm), with a particle size of 5 µm, from Waters (Ireland). Two mobile phases, A (0.1% of formic acid in ultra-pure water) and B (0.1% of formic acid in HPLC-grade acetonitrile) were used, at a flow rate of 0.5 mL min^{-1}. The oven temperature was kept at 45 °C, and the analysis period was 45 min. The detection wavelengths used for the quantification of hydroxybenzoic acids (protocatechuic and hydroxybenzoic), epicatechin and hydroxycinnamic acids (p-coumaric and ferulic acids) were fixed at 254, 275 and 315 nm, respectively (Supplementary Table 1).

Phenolic standards including chlorogenic, 4-hydroxybenzoic, vanillic, syringic, protocatechuic, syringaldehyde (3,5-dimethoxy-4-hydroxybenzaldehyde) and caffeic acids, as well as vanillin, all purchased from Acros Organics (Belgium). Rutin hydrate, p-coumaric acid, (-)-epigallocatechin gallate, (+)-catechin hydrate, kaempferol and (-)-epicatechin were from Sigma-Aldrich (Germany). Quercetin was supplied by Phytolab (Germany). Gallic acid hydrate and resveratrol by TCI (Belgium). Sinapic acid and myricetin by Fluka (Germany). Ferulic acid was from EDQM (France). All phenolic standards had a purity grade of at least 97.0%, except for (+)-catechin hydrate (≥ 96.0%), quercetin, 4-hydroxybenzoic acid and ferulic acid (≥ 95%), and rutin hydrate (≥ 94%). Absolute ethanol (> 99.8%) and HPLC-grade acetonitrile were from Honeywell (Germany). Formic acid (≥ 99.9%) was obtained from VWR Chemicals (Belgium). Ultra-pure water (18 MΩ·cm) was produced using a Simplicity UV ultrapure water system (type 1) from Millipore (USA).

Agronomic assessment

Nitrogen concentration

Samples previously weighed were digested at 420 ºC in a Velp Scientifica digester (DK 8S Digester Heater, Velp Scientifica, Italy) together with potassium sulphate to elevate the boiling temperature of the sulphuric acid and using selenium as a catalyst. The aqueous ammonium sulphate produced during the reaction was titrated in a distillation and titration unit (Model UDK 152, Velp Scientifica) by adding sodium hydroxide with a concentration of 11.2 mol L^{-1}. After, the ammonia gas was condensed, and boric acid was added to form an ammonium borate complex. Bromocresol

green and methyl red indicators were used for the quantification of total nitrogen.

Phosphorus concentration

To quantify phosphorus in samples, a calibration curve ($y = 0.6556x + 0.0065, R^2 = 0.999$) was established using monobasic potassium phosphate (KH_2PO_4) from 0 to 0.6 mg L^{-1}. Samples were extracted with Olsen reagent in a proportion of 0.1 g of sample to 2 mL of reagent, shaken at 200 rpm on an orbital shaker (New Brunswick Innova 2100, Canada) for 30 min and centrifuged (Eppendorf Centrifuge 5430 R, Germany) at 2500 rpm for 10 min. After, the supernatant was filtered using a Whatman filter paper with an 8 µm pore size, mixed with water, incubated for 30 min and read at 882 nm.

Spectroscopic analysis

Attenuated Total Reflectance – Fourier Transform Infrared Spectroscopy (ATR-FTIR) of the polysaccharides were obtained with a Perkin Elmer Spectrum Two, coupled with a Diamond ATR accessory (DurasamplIR II, Smiths Detection, UK). Thirty-two scans were acquired in transmittance mode in the range of 4000—400 cm^{-1}, with a wavenumber resolution of 1 cm^{-1}. Blanks were performed at the beginning of the measurements to remove background noise, correcting the baseline interference and all samples analysed in triplicate. Also, correlations were performed using the Perkin Elmer software to establish the association between the polysaccharides extracts and four standards, agar, agarose, carrageenan and k-carrageenan.

Statistics

Values are expressed as an average of three replicates ± standard deviation. SPSS 30 software was used to perform a One-Way ANOVA analysis with homogeneity of variances. Statistical variance was also determined using the post hoc Tukey's b test, with a significance level of $p < 0.05$. STATISTICA 10 software was used to perform the 3D plots. PCA plots were performed using the MVSP 3.22 software.

Results

Optimization of protein and phycoerythrin extraction

Tridimensional plots were produced to optimize the extraction methodology of protein and PE from these selected three red macroalgae. This assessment was performed varying Timatic extraction cycles between 6, 12 and 18 with fresh biomass from 100, 200 and 400 g fresh weight. These evaluations demonstrated that the highest concentrations of protein and PE can be expected from the red macroalga *G. lanceola* collected at the offshore fish farms. According to the surface plots illustrated in Fig. 2, this macroalga protein content exceeds 3000 mg L^{-1} when performing extractions with higher fresh biomass content and number of extraction cycles. Conditions to extract higher concentrations (exceeding 240 mg L^{-1}) of PE from the same biomass, are similar but using a lower number of cycles. The alga *A. taxiformis* showed the same pattern as *G. lanceola* for protein concentration, reaching more than 350 mg L^{-1}. *A. taxiformis* PE extraction demonstrated a different behavior, obtaining higher concentrations when higher fresh biomass and number of extraction cycles are used, reaching 15 mg L^{-1}. However, lower number of extractions cycles, using higher fresh biomass, only slightly influences the PE extraction, reaching values of 13 mg L^{-1}. Samples collected along the southern shores of Madeira had the lowest PE values, as well as the highest discrepancy between total protein content and PE. Surface plot for *N. elminthoides* demonstrated that it is not necessary to reach the higher fresh biomass content and number of extraction cycles to reach the highest total protein concentration, which exceeds 300 mg L^{-1}, being enough the lowest cycle number and 300 g of fresh biomass. The extraction of PE higher concentration follows the trend of first two cases, meaning that a higher fresh weight and number of extraction cycle is beneficial, reaching more than 50 mg L^{-1} under these conditions.

Biorefinery

The adopted biorefinery methodology allowed the sequential extraction of protein, bioactive extract and finally polysaccharides. Two residues, one liquid and one solid were also quantified due to their direct relation to the original biomass. To facilitate the comparison between different compounds, all were presented in grams per 100 g of dry weight (g $(100\ g)^{-1}$ dw), as presented in Fig. 3.

Total soluble protein extracted from the selected red macroalga varies between 1.35 ± 0.09 g $(100\ g)^{-1}$ with the *A. taxiformis* 0.5-L (vessel volume used in Timatic extrator) to 6.25 ± 0.59 g $(100\ g)^{-1}$ dw with the *G. lanceola* 2-L. Comparing protein extracts, not considering the extraction vessel volume used in the Timatic extractor, *G. lanceola* presents on average the highest protein content, 5.94 g $(100\ g)^{-1}$ dw. The bioactive extract varied between 4.08 ± 0.13 and 11.81 ± 0.31 g $(100\ g)^{-1}$ dw in the *N. elminthoides*. Namely the 0.5-L vessel resulted in a lower yield than the 1-L vessel. *A. taxiformis* presents the highest content of bioactive extract, 8.99 g $(100\ g)^{-1}$ dw, disregarding the Timatic extraction vessel used. The polysaccharides content extracted from macroalgae biomass varied from 0 g $(100\ g)^{-1}$ dw in *N.*

Asparagopsis taxiformis – Protein (mg L^{-1})

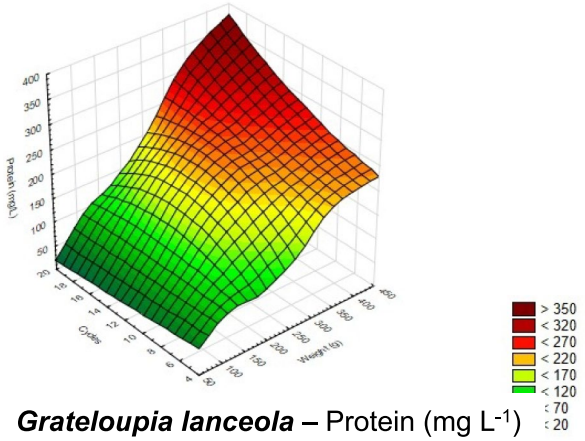

Asparagopsis taxiformis – Phycoerythrin (mg L^{-1})

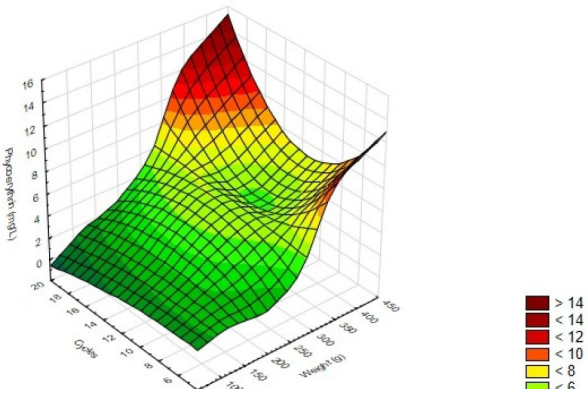

Grateloupia lanceola – Protein (mg L^{-1})

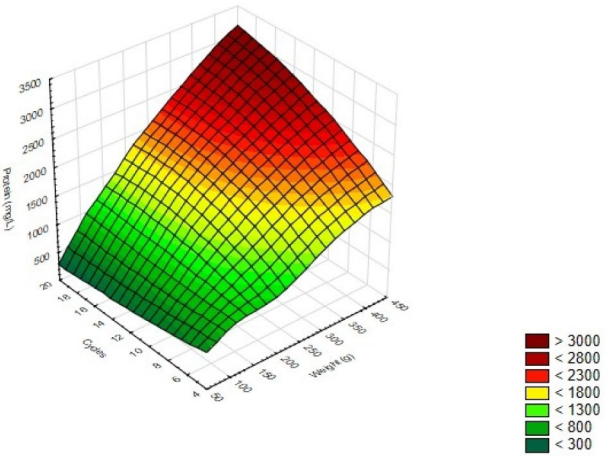

Grateloupia lanceola – Phycoerythrin (mg L^{-1})

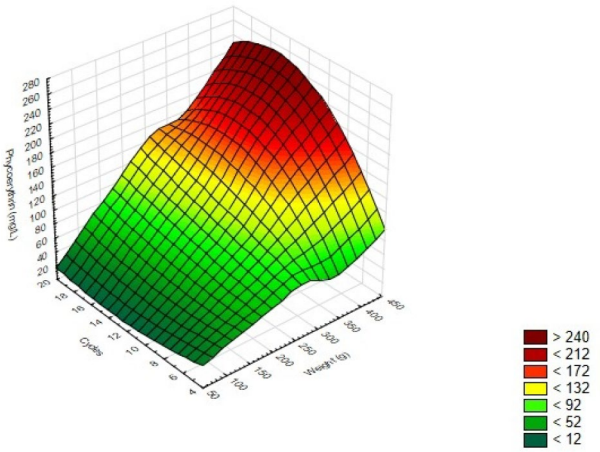

Nemalion elminthoides – Protein (mg L^{-1})

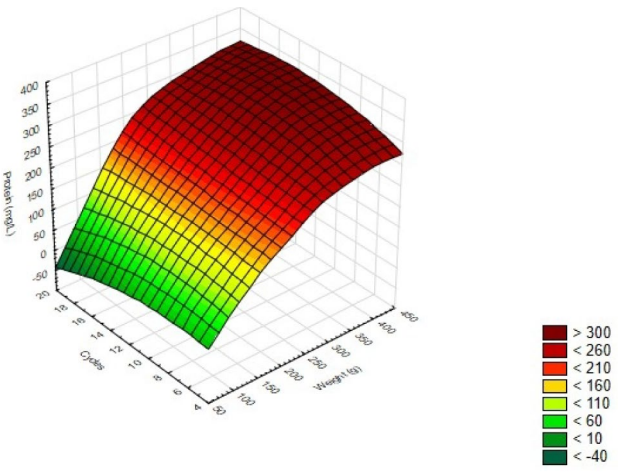

Nemalion elminthoides – Phycoerythrin (mg L^{-1})

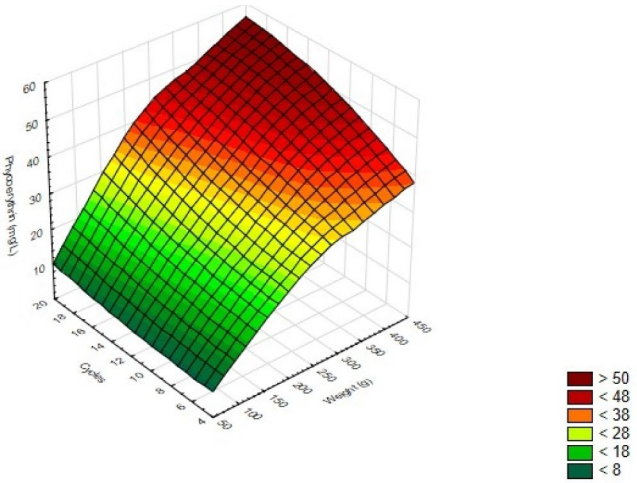

Fig. 2 3D plots relating the number of cycles (X) of the Timatic pressure extractor with the fresh weight (Y) of the biomass to assess its relationship with protein (Z) and phycoerythrin (Z) in the primary extract derived from the 3 red macroalgae, performed with STATISTICA 10.0

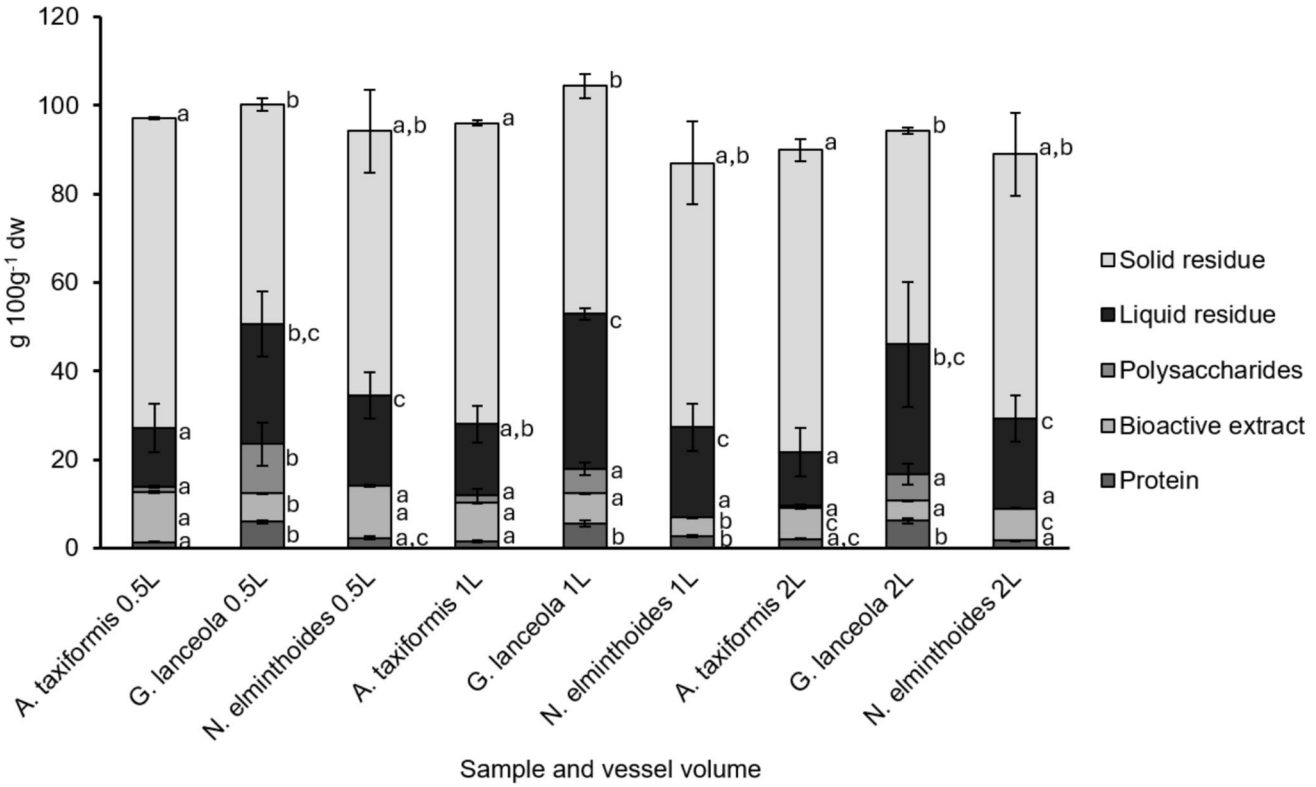

Fig. 3 Stacked columns graphic for biorefinery products extracted from the 3 red macroalgae, varying the vessel used in the Timatic pressure extractor for scale up evaluation ($n=3$ replicates ± standard deviation). Different letters within the same parameter indicate significant differences ($p<0.05$) determined using Tukey b test

elminthoides independently of the extraction vessel used and 11.13 ± 4.85 g (100 g)$^{-1}$ dw in *G. lanceola* 0.5-L. *G. lanceola* presents the highest polysaccharides content of 7.47 g (100 g)$^{-1}$ dw. The resulting liquid residue content, derived from the polysaccharide extraction, varied between 12.13 ± 5.50 g (100 g)$^{-1}$ dw for the *A. taxiformis* 2-L and 35.10 ± 1.29 g (100 g)$^{-1}$ dw for the *G. lanceola* 1-L. In relation to the averages of liquid residue extraction, *G. lanceola* presents the highest concentration, 30.54 g (100 g)$^{-1}$. Finally, the solid residue shows minimum content in the *G. lanceola* 2-L, 48.18 ± 0.77 g (100 g)$^{-1}$ dw, and the maximum in *A. taxiformis* 0.5L, 70.02 ± 0.77 g (100 g)$^{-1}$ dw.

Protein and phycoerythrin quantification

Protein extracted from red macroalga samples are present in Fig. 4 to enable a reasonable comparison between extraction concentrations.

The first extract performed with phosphate buffer solution using the Timatic extractor is the crude extract, which was only measured the protein content without any concentration endeavor. Crude protein extract demonstrated the lowest concentration with *N. elminthoides*, 77.63 ± 3.02 mg L^{-1}, and *G. lanceola* the highest, 922.75 ± 87.53 mg L^{-1}, both using a 2-L vessel in the Timatic extractor. Highest average concentration, not considering the vessel used in the Timatic extractor, was obtained with the *G. lanceola*, 878.79 mg L^{-1} of soluble protein. When comparing the concentration of the precipitated protein using 30% ammonium sulphate, the range was between *A. taxiformis* 0.5-L, 457.34 ± 85.92 mg L^{-1}, and *G. lanceola* 2-L, 1193.71 ± 252.64 mg L^{-1}. The highest average concentration was 787 mg L^{-1} for the *G. lanceola*. Considering the highest amount of ammonium sulphate used (90%) to precipitate protein, lowest concentration was observed in *A. taxiformis* 0.5-L, 847.20 ± 43.63 mg L^{-1}, and the highest with *G. lanceola* 1-L, 1844.49 ± 85.90 mg L^{-1}. The highest average protein concentration, 1776.86 mg L^{-1}, was obtained from *G. lanceola*. Since the highest protein concentration was observed in its extracts, possibly there is still a small fraction of protein left in the supernatant. So, the *G. lanceola* supernatant still had between 86.52 ± 11.50 mg L^{-1} and 260.43 ± 41.48 mg L^{-1} solubilized protein (different vessel volume). The remaining supernatants from *A. taxiformis* and *N. elminthoides*, had a protein concentration below the limit of quantification (2.5 mg L^{-1}).

The concentration and purity of the PE extracted from *A. taxiformis* are compared in Fig. 5, between the crude

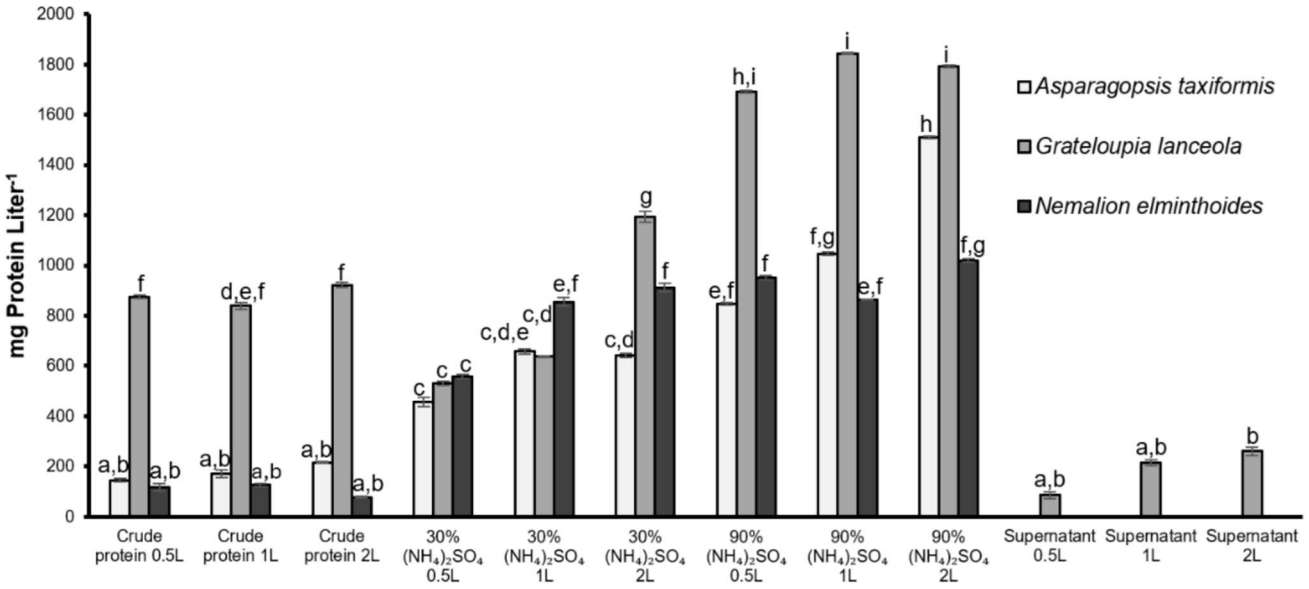

Fig. 4 Comparing the concentration of crude protein, the two gradients selected (30 and 90%) of ammonium sulphate, $(NH_4)_2SO_4$, to precipitate protein and the supernatant for efficiency assessment ($n = 3$ replicates ± standard deviation). Different letters indicate significant differences ($p < 0.05$) determined using Tukey b test

extract, ammonium sulphate (30 and 90%) precipitation and supernatant.

Also, a comparison was performed taking into consideration the scaling up of the process, using the Timatic equipment with 3 different vessels (0.5-L, 1-L and 2-L). The crude extract exhibited a similar concentration using the different vessels, achieving the maximum concentration (4.42 mg L^{-1}) and purity (0.09) using the 2-L vessel. The maximum concentration of PE was found in the 30% ammonium sulphate precipitate, using the 0.5-L vessel (79.13 mg L^{-1}) with a purity of 0.63. The 1-L vessel within the same precipitation condition, reached maximum purity, as confirmed with the fluorescence data (Fig. 6).

In Fig. 7, it can be observed that the crude extract from the *G. lanceola* was also similar between the different vessels used, showing its maximum concentration using the 0.5-L vessel (50 mg L^{-1}).

Contrarily, maximum purity within the crude extracts was achieved in the 1L vessel (0.64). The highest PE concentration (216 mg L^{-1}) and purity (2.05) was obtained using the 0.5-L vessel and precipitating with 90% ammonium sulphate. A discrepancy between the spectrophotometric method and fluorescence to ascertain the highest purity was observed, in which using the fluorescence data (Fig. 6), the highest purity was when using the same percentage of salt to precipitate the PE but using the 1-L vessel. In Fig. 8, a similar comparison can be observed for *N. elminthoides*, in which a different PE concentration in the crude extract was obtained, with the highest concentration (25.21 mg L^{-1}) and purity index (0.49), achieved using the 0.5-L vessel. The highest concentration was observed using the 2L vessel and 30% ammonium sulphate precipitation (187.35 mg L^{-1}) but not with the highest purity index which was obtained with the 1-L vessel and 90% ammonium sulphate precipitation (1.57), also confirmed with the fluorescence data (Fig. 6).

The FPLC purification produced the best results regarding the purification of *N. elminthoides* 90% 1-L extract, which increased the purity index from 1.570 to 7.546, the PE concentration from 167.305 to 308.628 mg L^{-1} but with a very low recovery percentage, 0.356% (Table 1). *Grateloupia lanceola* 90% 0.5-L extract did not increase its purity index, passing from 2.054 to 1.947 but increased the PE concentration, from 216 to 347.398 mg L^{-1}. For *A. taxiformis* 30% 1-L extract it was not possible to increase its purity index or its PE concentration using the methodology described.

A correlation between the concentration of protein and PE was established for each red macroalga species studied, during optimization of the protein and PE extraction in Timatic, as shown in Fig. 9. *A. taxiformis* shows the lowest correlation in this study ($R^2 = 0.83$) being also the biomass with less concentration of PE, presenting an average of 41 times lower concentration of PE than the undifferentiated protein in the initial extraction optimization. The highest correlation was found in *G. lanceola* ($R^2 = 0.96$), the highest source of protein and PE in this work, presenting an average of 18 times lower PE concentration compared to the undifferentiated soluble protein. Also, *N. elminthoides* presented a correlation between PE and protein of $R^2 = 0.92$, and an

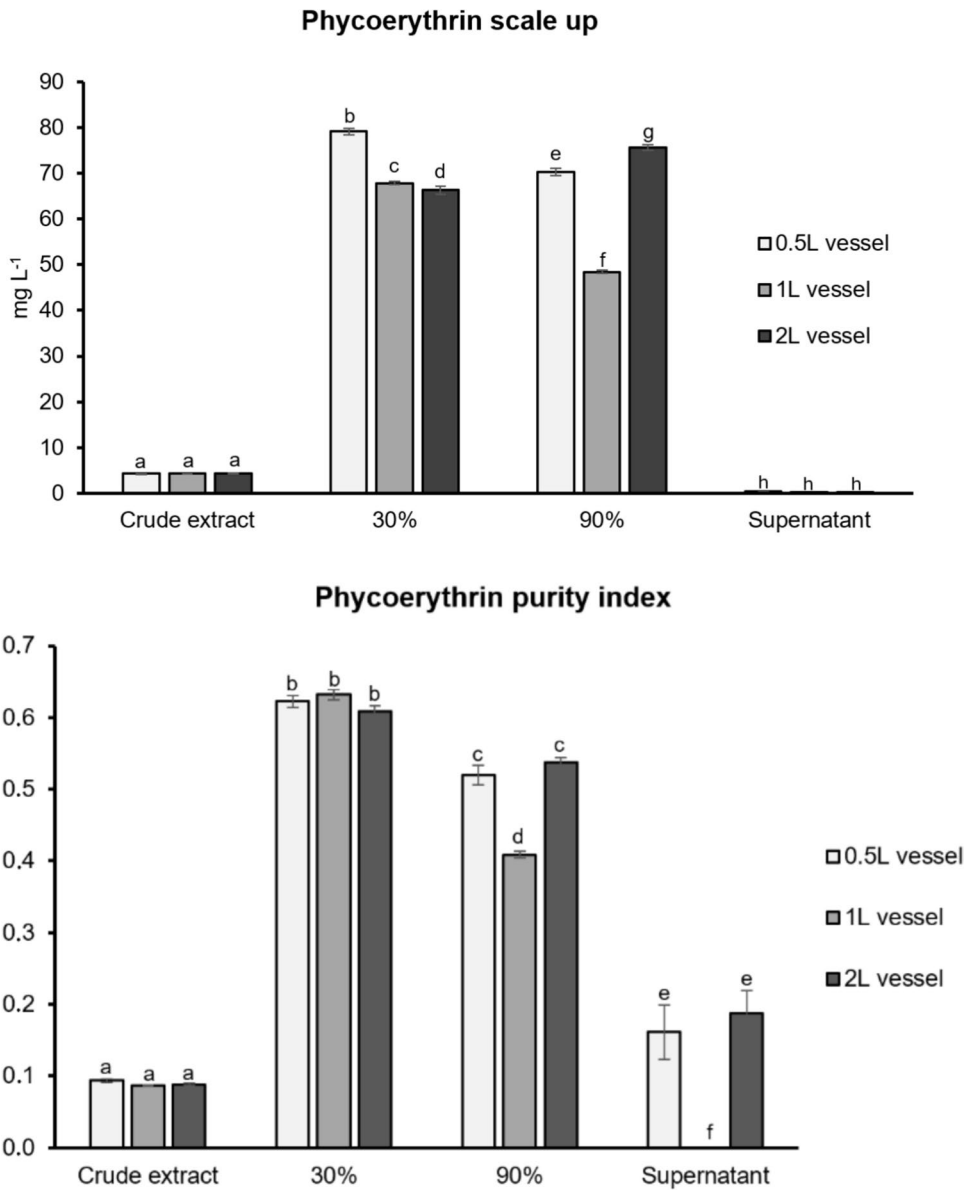

Fig. 5 Scaling up the phycoerythrin extraction of *A. taxiformis* using different extraction vessels with the Timatic extractor and determining the purity index of the extracts ($n = 3$ replicates ± standard deviation). Different letters indicate significant differences ($p < 0.05$) determined using Tukey b test

average of 6 times less PE. Although this is a more favorable data, *N. elminthoides* does not reach the same PE concentration as *G. lanceola* in terms of mg L^{-1}.

The precipitation with 90% ammonium sulphate concentrated the PE four times, from 50 mg PE L^{-1} in the crude extract to 216 mg PE L^{-1} (0.5-L vessel) in the *G. lanceola*. Although the FPLC was efficient to concentrate PE from 216 to 347 mg PE L^{-1}, it failed to increase the purity index, which decreased from 2.054 to 1.947, respectively. This could be due to similar size proteins going out at the same time as PE through the Size Exclusion Column (SEC, 16/60 Sephacryl S-200 HR).—*Nemalion elminthoides* had a maximum concentration of 187 mg PE L^{-1} using the 2-L vessel and 30% ammonium sulphate precipitation, obtaining almost a 10 times increase of PE in comparison with the crude extract (19 mg PE L^{-1}). Still, we have not used this extract for further purification since purity index was low. On the other hand, the fraction precipitated with 90% $(NH_4)_2SO_4$ (1-L vessel), showed a 167 mg PE L^{-1} concentration and a purity index of 1.570, increased after FPLC, reaching 309 mg PE L^{-1} and a purity index of 7.546. This is an indication that this procedure is adequate to PE purification derived from this macroalga, since non-targeted proteins have different solubility and/or size when compared to PE of *N. elminthoides*.

Total phenolic content (TPC)

The TPC was measured both in the bioactive extracts derived from the 2nd biorefinery step and in the extracts

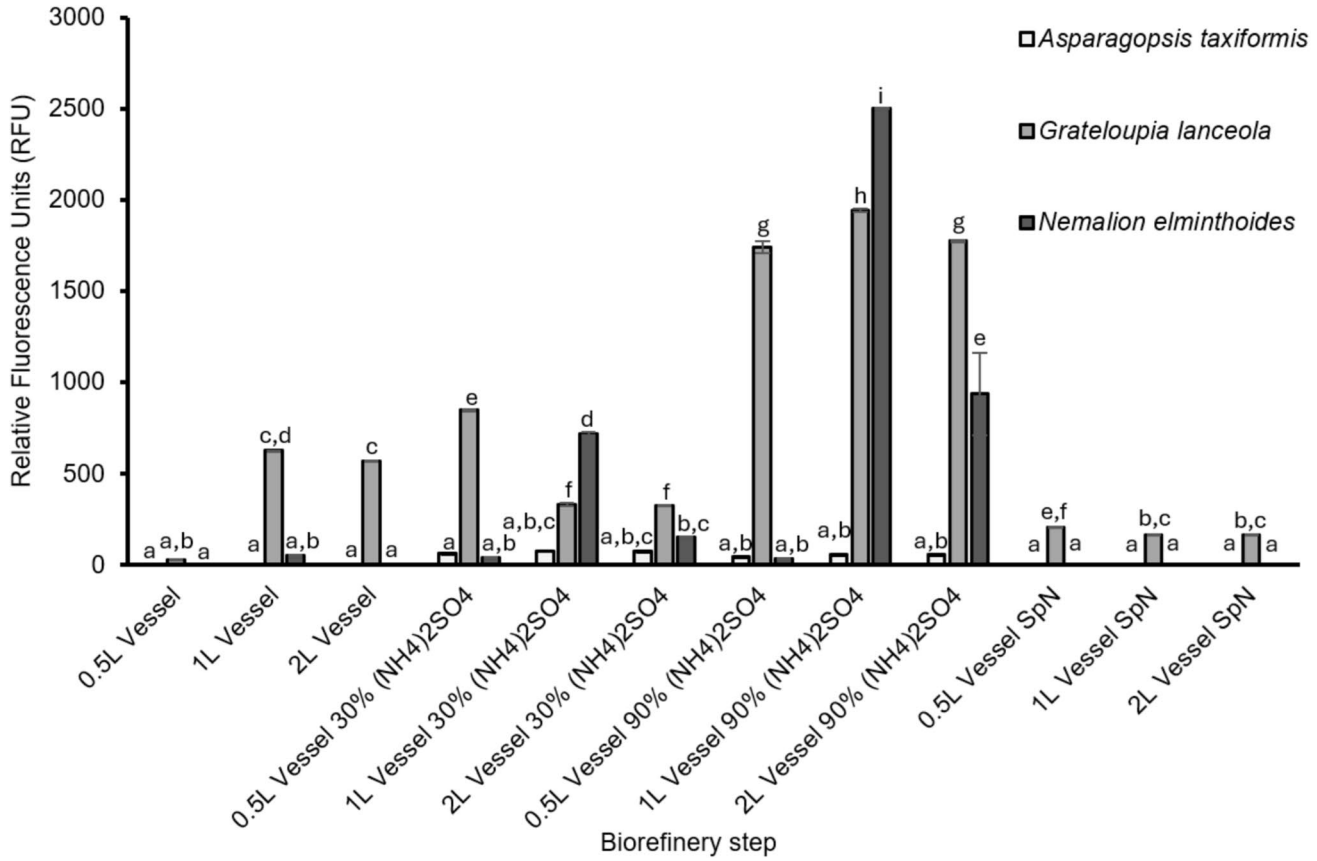

Fig. 6 Fluorescence assessment, exciting the phycoerythrin with 550 nm and detecting the emission at 576 nm ($n=3$ replicates ± standard deviation). Scaling up the phycoerythrin extraction using different extraction vessels with the Timatic extractor and determining the Relative Fluorescence Units (RFU) of the crude extracts, precipitated extracts (30 and 90% ammonium sulphate) and the supernatant (SpN). Different letters indicate significant differences ($p<0.05$) determined using Tukey b test

derived directly from the fresh biomass, without extracting the protein first, so it would be possible to compare the characteristics of this extract directly and follow the adopted biorefinery strategy (Fig. 10).

The TPC from *A. taxiformis* varied from 1.42 ± 0.08 to 1.9 ± 0.12 mg GAE g^{-1} dw bioactive extract. The direct extraction presented a lower concentration of TPC (1.38 ± 0.22 mg GAE g^{-1} dw) in comparison to extracting from the residual biomass. The highest concentration was found in the extract obtained from the 2L Timatic vessel. In the *G. lanceola*, TPC varied from 2.31 ± 0.01 to 5.16 ± 0.06 mg GAE g^{-1} dw, being the concentration of the direct extraction between this interval, 4.31 ± 0.21 mg GAE g^{-1} dw. In the *N. elminthoides*, this was not the case, demonstrating the direct extraction a higher TPC concentration, 2.13 ± 0.17 mg GAE g^{-1} dw than the interval concentration which resulted extracting from the residual biomass, 1.69 ± 0.04 and 2.12 ± 0.12 mg GAE g^{-1} dw.

Bioactive extracts analytical assessment

The HPLC assessment showed that the hydroxybenzoic acids highest values were 23.432 ± 0.932 µg g^{-1} dw for protocatechuic acid and 31.029 ± 0.790 µg g^{-1} dw for hydroxybenzoic acid (Table 2).

Epicatechin presented a maximum value of 573.156 ± 18.594 µg g^{-1} dw in the extract derived from the 2L vessel for *G. lanceola*. For the hydroxycinnamic acids, p-coumaric presented a maximum value of 28.975 ± 0.474 µg g^{-1} dw and ferulic acid 8.115 ± 0.138 µg g^{-1} dw. For the remaining phenolic acids assessed, gallic acid, catechin, chlorogenic acid, caffeic acid, vanillic acid, epigallocatechin gallate, syringic acid, vanillin,

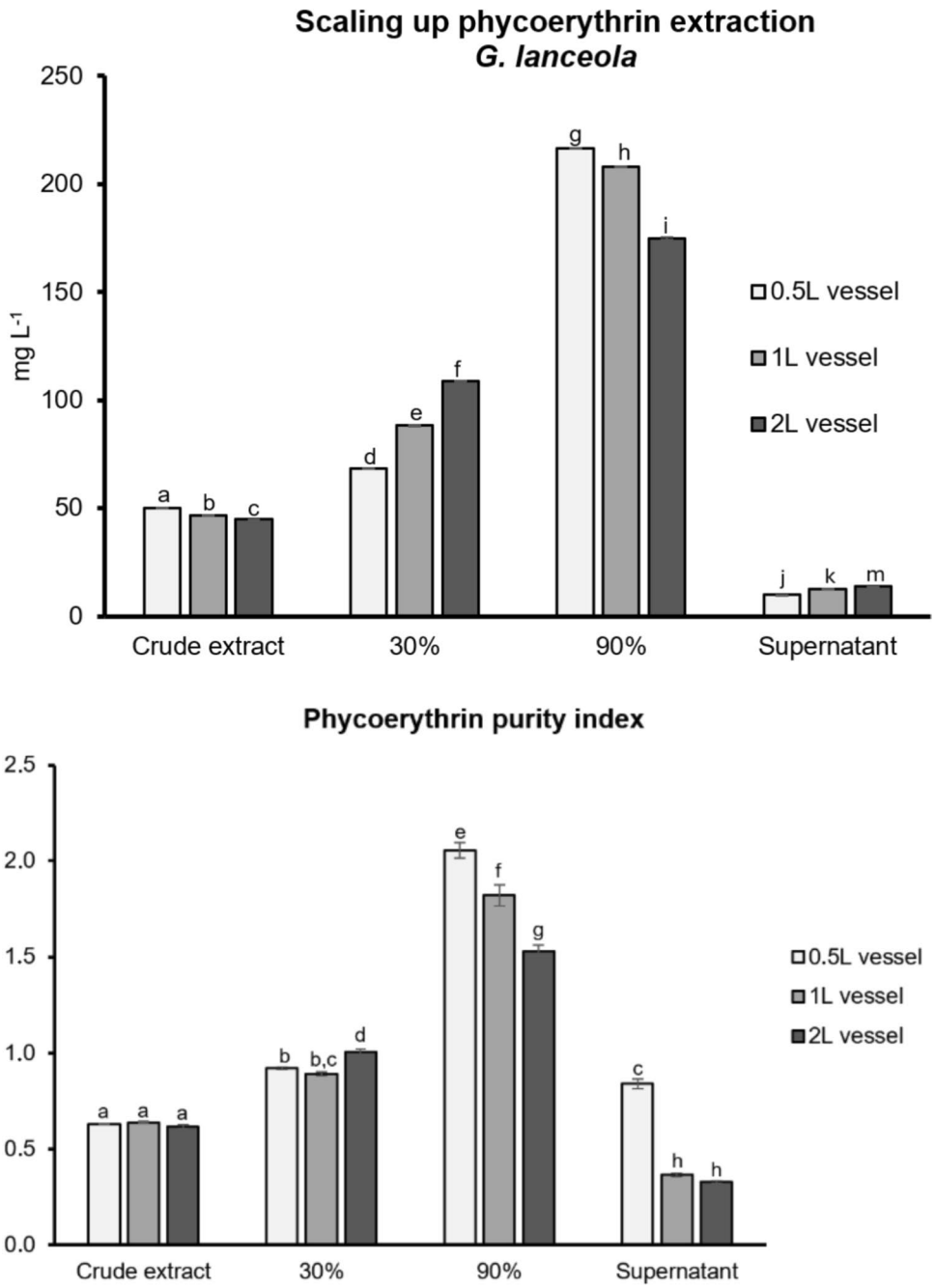

Fig. 7 Scaling up the phycoerythrin extraction of *G. lanceola* using different extraction vessels with the Timatic extractor and determining the purity index of the extracts ($n = 3$ replicates ± standard deviation). Different letters indicate significant differences ($p < 0.05$) determined using Tukey b test

syringaldehyde, rutin, sinapic acid, myricetin, resveratrol, quercetin and kaempferol, it was not possible to quantify in these samples.

Agronomic assessment

The nitrogen and phosphorus content of the 2 main residues of this biorefinery strategy, which includes the liquid residue from the polysaccharide's extraction and the final solid residue, a depleted dried biomass, generally known as algal cake, were assessed. The nitrogen content of the liquid residue varied from 6.507 ± 0 mg g^{-1} dw to a maximum value of 34.975 ± 0 mg g^{-1} dw (Table 3).

Nitrogen content in the solid residue varied from 17.282 ± 1.761 to 53.274 ± 3.134 mg g^{-1} dw (Table 4), which residues from *A. taxiformis* demonstrated the highest nitrogen concentration.

Phosphorus concentration in the liquid residues varied from 0.84 ± 0.091 to 139.457 ± 2.188 µg g^{-1} dw (Table 3). In the solid residues (Table 4) these values varied from

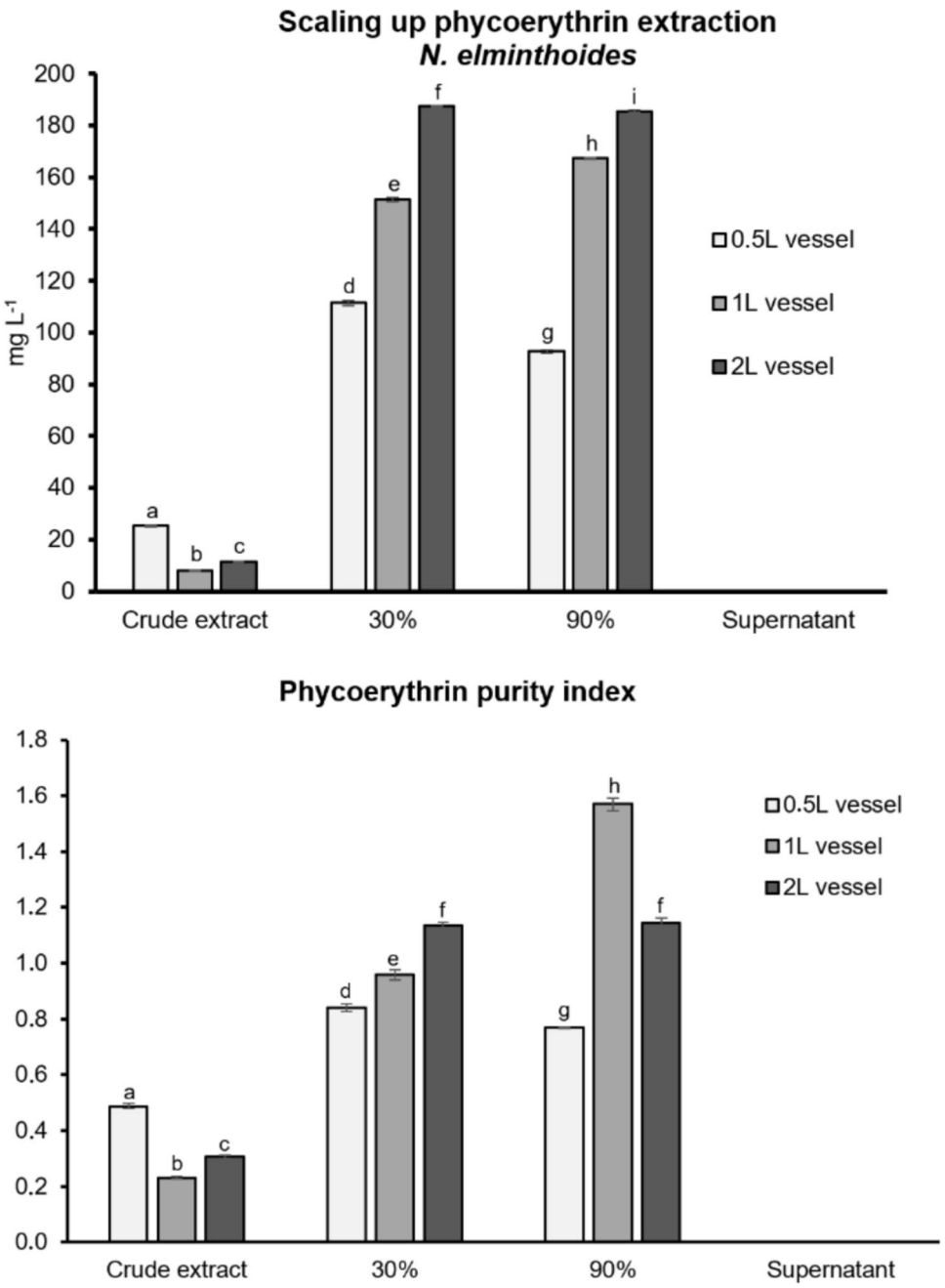

Fig. 8 Scaling up the phycoerythrin extraction of *N. elminthoides* using different extraction vessels with the Timatic extractor and determining the purity index of the extracts ($n = 3$ replicates ± standard deviation). Different letters indicate significant differences ($p < 0.05$) determined using Tukey b test

Table 1 Average values of the FPLC purification for phycoerythrin concentration

Macroalgae	Origin	Recovery PE (crude to precipitation) (%)	Purity index FPLC (OD_{565}/OD_{280})	Concentration PE FPLC (mg L^{-1})	Recovery PE (crude to FPLC (%)
A. taxiformis	2-L 30% $(NH_4)_2SO_4$	15.509	0.060	3.970	0.027
G. lanceola	0.5-L 90% $(NH_4)_2SO_4$	9.951	1.947	347.398	0.703
N. elminthoides	1-L 90% $(NH_4)_2SO_4$	16.029	7.546	308.628	0.356

$n = 3$ replicates

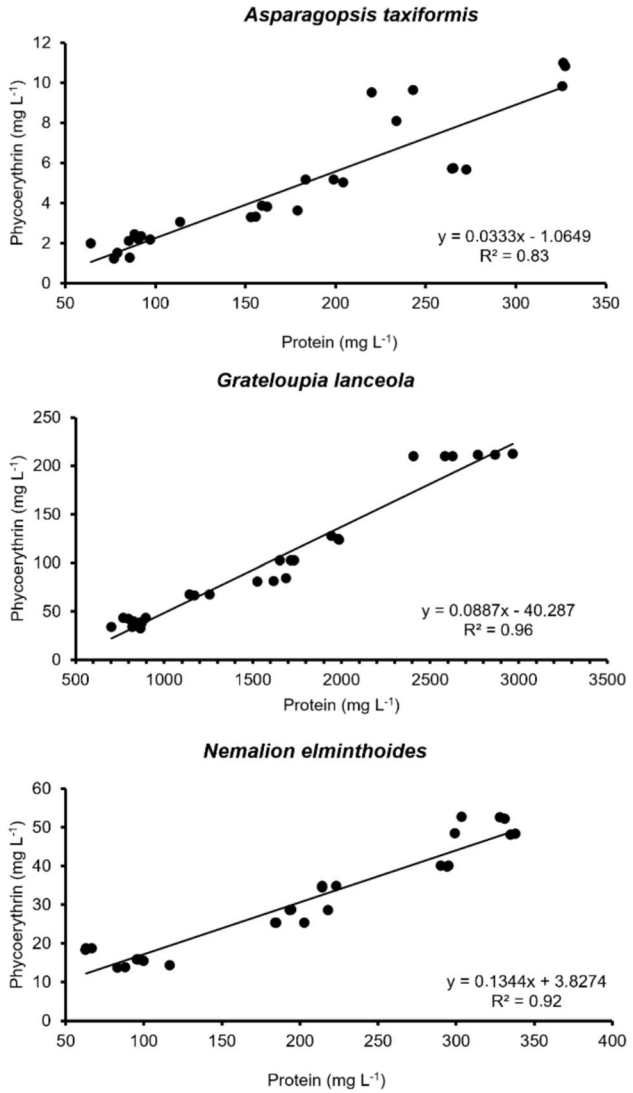

Fig. 9 Graphics correlating protein and phycoerythrin concentration derived from the optimization tests for the three red macroalgae

0.355 ± 0.034 to 86.107 ± 3.528 µg g^{-1} dw, presenting lower values than the liquid residue.

Spectroscopic analysis

By comparing the transmittance (%) versus wavenumber (cm^{-1}) profiles of polysaccharide extracts from macroalga biomass, distinct characteristic polysaccharide transmittance peaks can be observed. (Fig. 11), either directly obtained polysaccharides or a result of the cascade biorefinery approach.

Transmittance reduction at 694, 741 and 770 cm^{-1} are normally attributed to the bending of the skeleton of the pyranose ring, which is more visible in the standards, can also be observed in *G. lanceola* and *A. taxiformis* extracts. Bands observed at 805 cm^{-1} are a product of 3,6-anhydro-D-galactose-2-sulphate (DA2S), observed as a reduced shoulder in some samples but prominently present in *N. elminthoides*. Bands presented at 820 and 867 cm^{-1} imply the presence of D-galactose-6-sulphate (D6S) and at 825 cm^{-1} to D-galactose-2,6-disulphate (D2S, 6S) observable in the standards, *A. taxiformis* and *G. lanceola* polysaccharide extracts. Bands observed at 845 cm^{-1} are allocated to D-galactose-4-sulphate (G4S), visible at different extents in all samples and standards. Bands present at 928, 933 and shoulders at 1070 cm^{-1} are 3,6 anhydro-D-galactose (DA), found prominently in the extracts derived from 1 and 2-L vessels from *A. taxiformis*, 2-L vessel of *G. lanceola* and the direct extract of *N. elminthoides*. Bands between 1010 and 1030 cm^{-1} together with bands at 1150 cm^{-1} are carbon to carbon and carbon to oxygen stretching vibrations present in the pyranoid ring, common to all polysaccharides. Bands at 1210 and 1260 cm^{-1} are usually assigned to sulphate ester (S) observable in higher extend in the extracts derived from the 1-L vessel of *A. taxiformis*, 2-L vessel of *G. lanceola* and direct extract of *N. elminthoides*. The statistical correlation between the polysaccharide extracts and 4 standards of polysaccharides usually present in red macroalgae are present in Table 5. Correlation values varied from 0.52 to 0.69 when comparing the transmittance pattern between carrageenan and the polysaccharide extracts, being 1 the maximum value. Highest correlation value (0.69) was presented by *G. lanceola* from the direct extract followed by the polysaccharides extracted from the same macroalga using the 2-L vessel. For κ-carrageenan, the correlation values fell within the same range, with the highest correlations observed in the same extracts as those for total carrageenan. When comparing to agar and agarose standards, the correlation values are lower. For instance, agar varied from 0.36 to 0.49 which higher correlation was found within the polysaccharides extract of *G. lanceola* 2-L. Values for the comparison between agarose standard and polysaccharides extracted from the macroalga were even lower, varying from 0.27 to 0.41, which again higher values were found within the *G. lanceola* 2-L and direct extract.

PCA assessment

The PCA biplot (Fig. 12) shows a clear separation of the samples along Axis 1 (57.1%), which represents the major source of variance and primarily distinguishes the three macroalgae. Axis 2 (26.7%) captures secondary variation associated with extraction scale and process-specific effects. *G. lanceola* clusters consistently on the left side of Axis 1, with all scaled extractions grouped closely together, indicates high biochemical stability across processing volumes. Its conventional extraction (*G. lanceola*

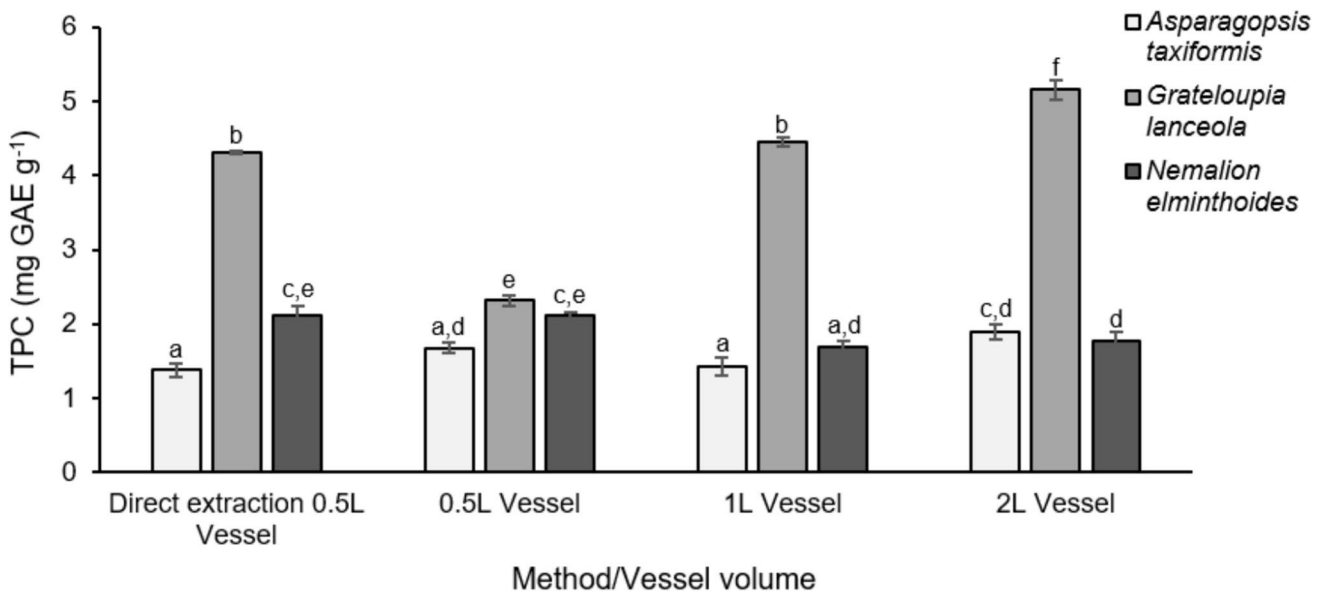

Fig. 10 Assessment of the total phenolics concentration (TPC) within the ethanolic (96%) extract ($n=3$ replicates ± standard deviation). For comparison purposes, a direct extraction was performed to relate between extracting from the residual biomass, after protein extraction. Also scaling up the ethanolic extract using different extraction vessels with the Timatic extractor. Different letters indicate significant differences ($p<0.05$) determined using Tukey b test

Table 2 Phenolic compounds concentration in ethanolic red macroalgae extracts

	Method/Vessel volume	Protocatechuic acid (μg g^{-1} dw)	Hydroxybenzoic acid (μg g^{-1} dw)	Epicatechin (μg g^{-1} dw)	p-coumaric acid (μg g^{-1} dw)	Ferulic acid (μg g^{-1} dw)
A. taxiformis	Direct extraction	n.d	6.027 ± 0.069^{a}	141.591 ± 1.338^{a}	16.121 ± 0.599^{a}	n.d
	0.5 L	n.d	$9.772 \pm 0.593^{b,c}$	124.142 ± 4.508^{b}	12.810 ± 0.534^{b}	n.d
	1 L	n.d	9.306 ± 0.415^{b}	167.737 ± 8.109^{c}	20.367 ± 0.569^{c}	n.d
	2 L	n.d	17.291 ± 0.429^{d}	422.842 ± 6.219^{d}	28.975 ± 0.474^{d}	n.d
G. lanceola	Direct extraction	n.d	20.719 ± 0.842^{e}	173.751 ± 3.722^{c}	n.d	n.d
	0.5 L	n.d	20.493 ± 0.817^{e}	251.351 ± 2.612^{e}	n.d	n.d
	1 L	n.d	15.155 ± 0.314^{f}	568.401 ± 9.820^{f}	7.737 ± 0.134^{e}	n.d
	2 L	n.d	$10.982 \pm 0.477^{c,g}$	573.156 ± 18.594^{f}	3.525 ± 3.058^{f}	n.d
N. elminthoides	Direct extraction	n.d	4.139 ± 0.179^{h}	51.567 ± 1.469^{g}	n.d	n.d
	0.5 L	23.432 ± 0.932^{a}	31.029 ± 0.790^{i}	107.149 ± 1.376^{h}	21.552 ± 1.146^{c}	8.115 ± 0.138^{a}
	1 L	15.833 ± 0.235^{b}	22.651 ± 0.572^{j}	63.521 ± 1.809^{g}	28.491 ± 0.317^{d}	8.047 ± 0.290^{a}
	2 L	8.983 ± 0.219^{c}	11.228 ± 0.332^{g}	28.653 ± 1.243^{i}	19.039 ± 0.658^{c}	7.114 ± 0.112^{b}

Different letters within the same parameter indicate significant differences ($p<0.05$) determined using Tukey b test. n.d – not determined. (μg g^{-1} dw, mean ± standard deviation) $n=3$ replicates

C) is positioned further left along Axis 1 due to the high contribution of polysaccharide quantification (Fig. 13). *A. taxiformis* forms a compact cluster on the far right of Axis 1, remaining clearly separated from both *G. lanceola* and *N. elminthoides*. Its conventional extraction (*A. taxiformis* C) shifts toward negative Axis 2 values, driven by its higher bioactive extract yield. The strong association of *A. taxiformis* with the right side of Axis 1 is largely influenced by the solid residue variable (Fig. 13), indicating a distinct compositional profile and lower solubilization efficiency compared with the other species. *N. elminthoides* occupies an intermediate region of the PCA space, with samples distributed across the center and lower portion of Axis 2. This dispersion reveals greater variability across scales and suggests that its extraction behavior is more sensitive to processing conditions. Similar to *A. taxiformis* C, the

Table 3 Nitrogen and phosphorus concentration within the liquid residue produced in the biorefinery method

Macroalgae	Vessel volume	Nitrogen (mg g^{-1} dw)	Phosphorus (μg g^{-1} dw)
Asparagopsis taxiformis	Direct extraction	13.484 ± 0^{a}	0.84 ± 0.091^{a}
	0.5 L	22.474 ± 1.946^{b}	139.106 ± 1.843^{b}
	1 L	23.597 ± 0^{b}	139.457 ± 2.188^{b}
	2 L	21.350 ± 1.946^{b}	92.194 ± 9.758^{c}
Grateloupia lanceola	Direct extraction	34.975 ± 0^{c}	4.283 ± 0.602^{a}
	0.5 L	15.898 ± 0^{a}	63.642 ± 2.769^{d}
	1 L	16.957 ± 1.836^{a}	19.634 ± 3.506^{e}
	2 L	17.487 ± 2.248^{a}	2.291 ± 0.105^{a}
Nemalion elminthoides	Direct extraction	14.098 ± 1.878^{a}	1.435 ± 0.092^{a}
	0.5 L	6.507 ± 0^{d}	139.026 ± 6.342^{b}
	1 L		
	2 L		

Liquid residue from *N. elminthoides* present a single value due to the very low concentration of polysaccharides in this macroalgae, which was considered neglectable. These residues were brought together from the 0.5, 1 and 2 L vessel, for comparison reasons. Different letters within the same parameter indicate significant differences ($p < 0.05$) determined using Tukey b test. (mean ± standard deviation) $n = 3$ replicates

Table 4 Nitrogen and phosphorus concentration within the solid residue produced in the biorefinery method

Macroalgae	Vessel volume	Nitrogen (mg g^{-1} dw)	Phosphorus (μg g^{-1} dw)
Asparagopsis taxiformis	Direct extraction	$43.872 \pm 0^{a,b}$	$2.706 \pm 0.204^{a,b}$
	0.5 L	52.229 ± 1.809^{c}	63.493 ± 2.906^{c}
	1 L	53.274 ± 3.134^{c}	61.799 ± 2.264^{c}
	2 L	$49.095 \pm 1.809^{b,c}$	28.576 ± 0.049^{d}
Grateloupia lanceola	Direct extraction	$36.598 \pm 0^{a,d}$	0.355 ± 0.034^{a}
	0.5 L	$30.498 \pm 0^{d,e}$	20.119 ± 0.037^{e}
	1 L	34.564 ± 1.761^{d}	5.746 ± 0.648^{b}
	2 L	$25.415 \pm 8.804^{e,f}$	$2 \pm 0.165^{a,b}$
Nemalion elminthoides	Direct extraction	$19.315 \pm 1.761^{f,g}$	9.993 ± 0.565^{f}
	0.5 L	17.282 ± 1.761^{g}	86.107 ± 3.528^{g}
	1 L		
	2 L		

Solid residue from *N. elminthoides* presents a single value due to the very low concentration of polysaccharides in this macroalgae, which was considered neglectable. These residues were brought together from the 0.5, 1 and 2 L vessels for comparison reasons. Different letters within the same parameter indicate significant differences ($p < 0.05$) determined using Tukey b test (mean ± standard deviation) $n = 3$ replicates

conventional extraction of *N. elminthoides* (*N. elminthoides* C) also appears in the negative range of Axis 2 due to its higher bioactive extract contribution.

Discussion

Optimization of protein and phycoerythrin extraction

The optimization of protein and PE extraction demonstrated strong species-specific responses to extraction cycles and biomass load. The tridimensional plots highlighted that both parameters significantly affect yields, though their influence varied across the three red macroalgae studied. *G. lanceola* showed the highest extraction potential under conditions of high biomass and increased cycle number, contrasting with PE extraction which peaked when using higher biomass but fewer cycles, suggesting that excessive processing may reduce pigment recovery, possibly through pigment degradation or saturation effects. For *A. taxiformis*, protein recovery followed a similar trend to *G. lanceola* and despite its protein potential, *A. taxiformis* exhibited the lowest PE concentrations and the largest disparity between protein and pigment yields, likely reflecting structural or biochemical differences. In *N. elminthoides*, maximum protein recovery was achieved without requiring high biomass or multiple

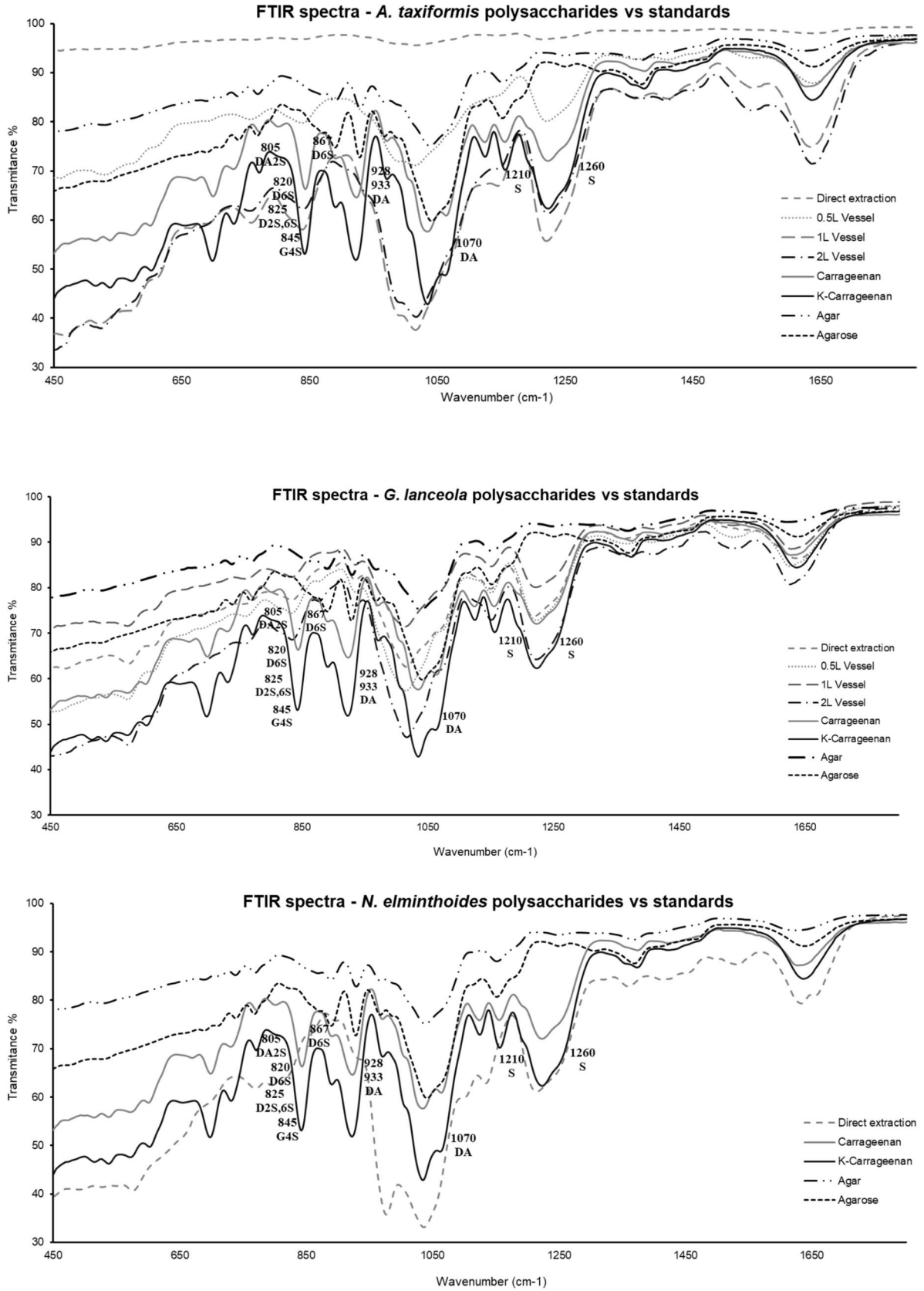

Fig. 11 FTIR spectra with wavenumber (cm^{-1}) vs transmittance (%) of the three macroalgae comparing with carrageenan, k-carrageenan, agar and agarose standards ($n = 3$ replicates)

Table 5 Transmittance pattern correlation between the polysaccharide extracts and 4 selected standards, using the Perkin Elmer software

Sample Name	Agar	Agarose	Carrageenan	K-Carrageenan
Asparagopsis taxiformis DE	0.39	0.31	0.58	0.57
A. taxiformis 0.5-L	0.36	0.27	0.62	0.61
A. taxiformis 1-L	0.38	0.30	0.64	0.64
A. taxiformis 2-L	0.41	0.33	0.63	0.63
Grateloupia lanceola DE	0.48	0.41	0.69	0.69
G. lanceola 0.5-L	0.47	0.40	0.66	0.66
G. lanceola 1-L	0.45	0.37	0.66	0.66
G. lanceola 2-L	0.49	0.41	0.68	0.68
Nemalion elminthoides DE	0.43	0.36	0.52	0.52

DE Direct Extraction; Correlation values are between 0 and 1. $n = 3$ replicates

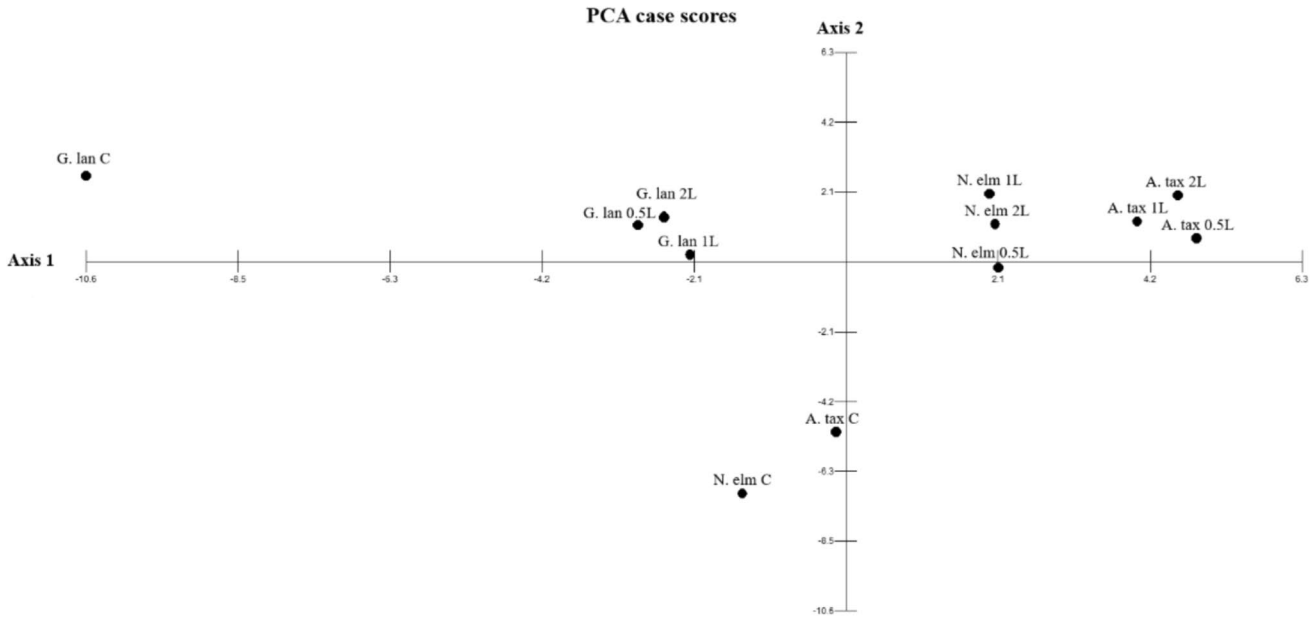

Fig. 12 PCA scatter plot for the case scores which includes analysis of the 16 variables (protein, phycoerythrin, bioactive extract, TPC, protocatechuic acid, hydroxybenzoic acid, epicatechin, p-coumaric acid, ferulic acid, polysaccharides, liquid residue, solid residue, nitrogen and phosphorus

cycles, highlighting efficient solubilization under milder conditions. PE extraction, however, followed a pattern where higher biomass and cycles enhanced recovery. This dual behavior positions *N. elminthoides* as a cost-effective protein source, though its pigment potential remains moderate. Collectively, these findings underscore the need to optimize extraction strategies according to species and target metabolite. While protein yields generally benefited from higher biomass and cycles, PE extraction was more sensitive to extraction intensity, with excessive cycling reducing yields in some cases.

Biorefinery

The concept of several compounds' extraction from the same biomass is considered a primary process and increases its efficiency in terms of natural resources. Concerning the dry weight (dw) results of each individual product obtained by applying this strategy, the orders are as follows: solid residue > liquid residue > bioactive extract > polysaccharides > protein > phycoerythrin. Although the cascade extraction approach enables the recovery of multiple high-value compounds, a substantial proportion of the biomass remains in low-value fractions, particularly solid and liquid residues. Furthermore, the careful selection and efficient recovery of environmentally benign (green) solvents are critical to ensure both

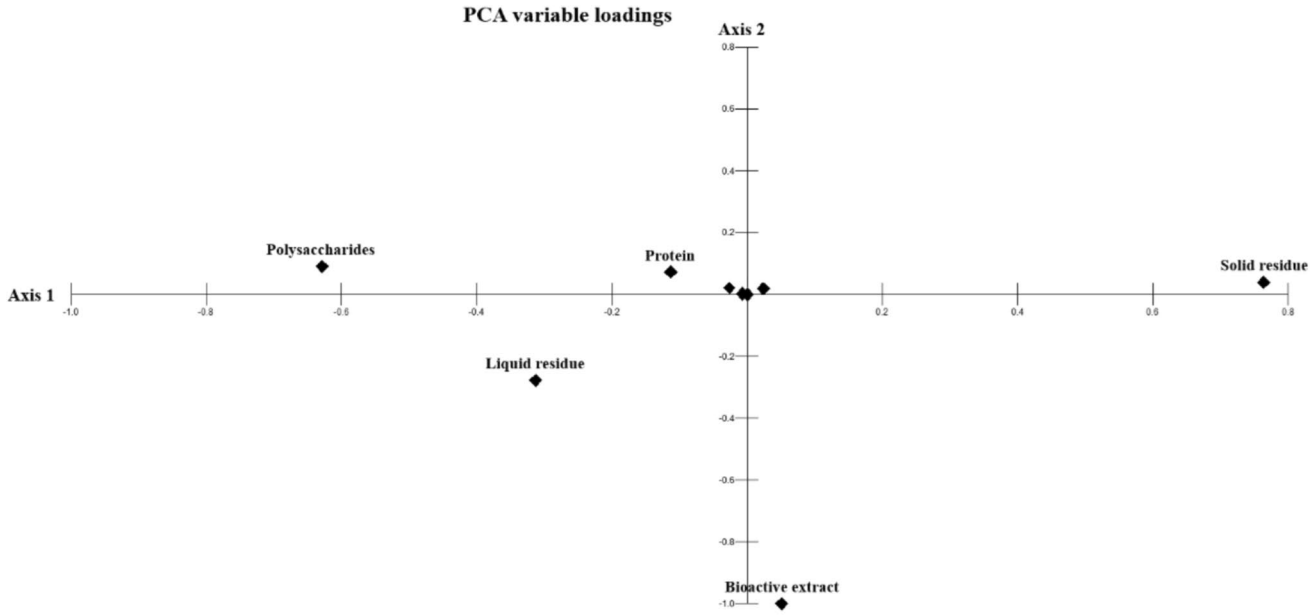

Fig. 13 PCA scatter plot for the 16 variables. Includes protein, phycoerythrin, bioactive extract, TPC, protocatechuic acid, hydroxybenzoic acid, epicatechin, p-coumaric acid, ferulic acid, polysaccharides, liquid residue, nitrogen (Liq. Res.), phosphorus (Liq. Res.), solid residue, nitrogen (Sol. Res.), phosphorus (Sol. Res.)

environmental sustainability and cost-effectiveness. It should also be noted that process scale-up often modifies extraction yields and efficiencies, which may, in turn, diminish the overall economic viability of the biorefinery system. Furthermore, conventional processing for single product extraction may not be economically feasible and multiple product production from the biomass could become an important strategy to reduce total expenditure (Koyande et al. 2019). Also, the low value residue obtained in this work could be further valued with alternative routes including the production of biochar and bio-oil (Alam et al. 2024) or even, a more profitable product, cellulose nanofibrils capable of filtering UV light (Jiang et al. 2025).

Comparing the 3 red macroalgae studied, *G. lanceola* extracts presented the highest concentration of extracted soluble protein and polysaccharides with *A. taxiformis* presenting the highest concentration of the bioactive extract. Several other works have been published concerning the new biorefinery methods applied to deconstruct red macroalgae biomass and produce marketable products. Baghel et al. (2016) extracted from *Gracilaria corticata* fresh biomass, collected from Diu, on western coast of India, primarily pigments, followed by crude lipids and agar, producing also bioethanol and quantifying the two main residues, a liquid rich water and a algae cake which suggest its use as a soil conditioner. Gomes-Dias et al. (2024) assessed dried red macroalgae from Spain and Portugal namely *Gelidium corneum*, *Gracilaria vermiculophyla* and *Porphyra dioica* targeting initially phycobiliproteins followed by a bioactive extraction, alkaline extraction for protein and hydrocolloid extraction. *A. taxiformis* was included in a previous study which produced a nutraceutical extract rich in iodine with antioxidant capacity, followed by crude lipids, polysaccharides and cellulose, suggesting an alternative biorefinery strategy for this red macroalga (Nunes et al. 2018).

Protein and phycoerythrin quantification

The extraction and fractionation of proteins and PE from the three red macroalgae revealed strong differences in yield, purity, and behavior during precipitation and purification. Overall, *G. lanceola* emerged as the most productive species, while *A. taxiformis* showed limited potential for pigment recovery despite measurable protein yields, and *N. elminthoides* demonstrated a favorable purification profile for PE. Protein concentration from crude extracts confirmed the species-dependent variability. Notably, residual protein in *G. lanceola* supernatants indicates incomplete recovery, suggesting that this species contains protein fractions with differing solubility. In contrast, proteins from *A. taxiformis* and *N. elminthoides* were almost fully precipitated, leaving supernatant concentrations below the quantification limit. The trends for PE extraction were more complex. In *A. taxiformis*, PE remained at low concentrations across all treatments, with maximum yield achieved after 30% ammonium sulphate precipitation. Purity

indexes were modest, and further purification attempts did not improve PE concentration, underlining the limited suitability of this species as a pigment source. By contrast, *G. lanceola* yielded the highest PE concentration with 90% ammonium sulphate precipitation. Scaling effects were evident, as vessel volume influenced both yield and purity. FPLC fractionation of the 90% precipitate increased PE concentration but did not enhance purity, which declined slightly. This outcome may reflect co-elution of proteins of similar sizes during size-exclusion chromatography, emphasizing the need for complementary purification approaches. In *N. elminthoides*, PE extraction showed intermediate behavior, with maximum concentration after 30% ammonium sulphate precipitation. However, purity indexes remained low under these conditions. Improved results were achieved with 90% precipitation in the 1-L vessel. Crucially, subsequent FPLC purification enhanced both concentration and purity, albeit with a low recovery rate. These results indicate that, despite lower initial PE levels compared with *G. lanceola*, *N. elminthoides* may be more amenable to high-purity PE recovery following chromatographic separation. Correlation analysis between protein and PE extraction highlighted species-specific relationships. *G. lanceola* showed the strongest correlation, reflecting its consistent high levels of both protein and PE, though PE remained approximately 18-fold lower than protein concentrations. *N. elminthoides* also showed a high correlation with a smaller discrepancy (sixfold difference), but its absolute PE yields were lower. *A. taxiformis* had the weakest correlation, consistent with its poor pigment content and recovery. Overall, the results reinforce *G. lanceola* as the most promising source of both protein and PE, with potential for scale-up, though purification bottlenecks remain. *N. elminthoides* offers a viable alternative for obtaining high-purity PE, particularly when coupled with chromatographic purification, despite lower recovery efficiency. In contrast, *A. taxiformis* appears more suited for protein recovery alone, given its poor PE yield and limited purification potential. These species-specific differences highlight the importance of tailored extraction and purification strategies, particularly when targeting high-value pigments for food, nutraceutical, or biotechnological applications. A similar effort was performed using harvested *Gracilaria tenuistipitata* from an aquaculture farm in Wanning, Hainan Province, China. Precipitation was achieved using 0.2 M ammonium sulphate and a STREAMLINE™ column, which was followed by purification by ion-exchange chromatography in a DEAE-Sepharose column (Zhao et al. 2020). The highest purity index obtained was 4.21, lower, but with a higher yield and recovery percentage when compared with our work.

Phycobiliproteins have been intensively studied over the years due to their applicability as a natural food colorant (Sekar and Chandramohan 2008). Nowadays, phycocyanin derived from *Arthrospira platensis* is approved as a natural blue food colorant under specific purity and safety conditions by the U.S. Food and Drug Administration (US FDA 2023). Both in EU and the US, phycoerythrin has not yet received formal authorization from major regulatory agencies as a food additive, where acceptance requires considerable scientific evidence (Vieira et al. 2025). Phycoerythrin pigment stability (Ghosh and Mishra 2020), green extraction methods (Xu et al. 2020) and generate comprehensive toxicological and safety data (George and John 2023) are still necessary to support their approval for food applications. The red macroalga *Gracilaria gracilis,* collected in Portugal mainland, has been included in this effort to substitute synthetic colorants by natural ones. Extraction by maceration resulted in the highest concentration of PE, 3.58 mg PE g^{-1}, compared to less efficient extraction methods (Pereira et al. 2020). In this work, values in crude extracts reached 4.16 and 3.39 mg PE per gram of dried sample for *N. elminthoides* and *G. lanceola* (data not shown), demonstrating the potential for the PE extraction and purification for commercial purposes. Since algae increase phycobiliproteins concentration when subjected to lower light conditions and when chlorophyll is not efficient for photosynthesis, collection from different locations and conditions explains the discrepancy between PE concentrations (Pereira et al. 2020).

Total phenolic content (TPC)

The TPC concentration showed different trends, depending on the macroalga. The *G. lanceola* shows a trend to increase concentration proportionally to the scaling up. Also, the sample from direct extraction presents higher concentration than the one obtained in the 0.5-L vessel extract, suggesting that some TPC is lost in the protein extraction step. *A. taxiformis* and *N. elminthoides* extracts did not follow this behavior, showing a random performance. The limited specificity of the Folin–Ciocalteu assay has been widely recognized as its principal limitation (Santos et al. 2019). TPC variability among the macroalgal extracts may be partly explained by the presence of non-phenolic compounds capable of reducing the Folin–Ciocalteu reagent, which includes several metabolites commonly present in macroalgae such as amino acids, protein, reducing sugars and ascorbic acid (Martínez-López and Tuohy 2023). Moreover, differences in cell wall composition and matrix complexity among species can influence solvent accessibility and the release of bioactive components including phenolic compounds (Santos et al. 2019).

Between the 24 macroalgae collected in Tenerife, Canary Islands, a broad concentration of TPC was observed, ranging from as low as 2.54 to 41.59 mg GAE g^{-1} dw which *Grateloupia imbricata* (Ruiz-Medina et al. 2022), same genus as *G. lanceola* showed similar TPC concentration, 4.19 and 4.31 GAE g^{-1} dw (direct extraction), respectively. This suggests that TPC concentrations are similar, within the same

genus, due to proximity and climatic similarities between these two neighboring archipelagos in the Atlantic Ocean.

Bioactive extracts analytical assessment

The concentration of protocatechuic acid was not detected in most bioactive extracts, only in *N. elminthoides*, in which it demonstrated to be inversely proportional to the scale up, diminishing its concentration as the volume of extraction vessel increases. This relationship can also be observed in *G. lanceola* and *N. elminthoides* for the hydroxybenzoic acid. Epicatechin presents a direct correlation with *A. taxiformis* and *G. lanceola* scale up but an indirect correlation in the case of *N. elminthoides*. The p-coumaric has a direct correlation with the scaling up of extraction volume in the case of *A. taxiformis* and an indirect correlation in the case of *N. elminthoides*. Ferulic acid only appeared in *N. elminthoides* and demonstrated an indirect correlation with the scaling up procedure. The biorefinery extracts from *N. elminthoides* obtained in this work were found to have a higher concentration of ferulic acid than the *Sargassum wightii* (0.08 ± 0.00 μg g^{-1}), *Ulva rigida* (0.21 ± 0.04 μg g^{-1}) and *Gracilaria edulis* (0.02 ± 0.00 μg g^{-1}), a brown, green and red macroalgae collected in India (Kumar et al. 2020). Still, vanillin was not detected in this work, but it was present in *S. wightii* (0.22 ± 0.07 μg g^{-1}), *U. rigida* (0.19 ± 0.06 μg g^{-1}) and *G. edulis* (0.39 ± 0.01 μg g^{-1}) (Kumar et al. 2020). A methanolic extract (60%) of the brown macroalga *Himanthalia elongata* collected in Ireland, presented a higher concentration of ferulic acid (17.6 ± 0.85 μg g^{-1}) and considerable concentrations of gallic acid, chlorogenic acid, caffeic acid, myricetin and quercetin (Rajauria 2018) which was not observed in our extracts. Also, brown macroalgae are known to possess more phenolic compounds, especially phlorotannin's, than green and red macroalgae (Holdt and Kraan 2011). Phenolic compounds are an extensive group of secondary metabolites which defend against infections, wounds, and environmental attacks (Santos et al. 2019). Biochemical discrepancies are known to be influenced by several factors including abiotic factors, different species, hydrodynamics, sample processing and extraction procedure.

Agronomic assessment

In this work, residues from *A. taxiformis* demonstrated the highest nitrogen concentration. Other works (Vega et al. 2020) which collected red macroalgae show around 20 to 30 mg g^{-1} dw. Solid residues derived from the *A. taxiformis* biorefinery tend to present higher concentration values, favouring the purpose of using these residues for biofertilization purposes.

Higher phosphorus concentration is present in liquid residues of *A. taxiformis* and *N. elminthoides*, higher than solid residues. It has already been demonstrated that macroalgae residues have the potential of being used as biofertilizers. Strawberry and corn crops were successfully fertilized with varying concentrations of residual biomass originated from the agar–agar extraction industry from Kenitra (Morocco) using the red macroalga *Gelidium sesquipedale* (Errati et al. 2022).

Spectroscopic analysis

The FTIR analyses confirmed the presence of characteristic carrageenan and agar related functional groups in the polysaccharide extracts from the three red macroalgae, though species-specific differences were evident. Transmittance reductions at 694, 741, and 770 cm^{-1}, associated with pyranose ring skeletal vibrations, were more prominent in the carrageenan standards but attenuated in *G. lanceola* and *A. taxiformis* extracts, suggesting partial structural modification or lower relative abundance of these moieties. Bands at 805 cm^{-1}, attributed to 3,6-anhydro-D-galactose-2-sulphate (DA2S), were most clearly expressed in *N. elminthoides*, consistent with its known polysaccharide composition. In contrast, absorptions at 820 and 867 cm^{-1} (D-galactose-6-sulphate, D6S) and at 825 cm^{-1} (D-galactose-2,6-disulphate, D2S,6S) were evident in carrageenan standards as well as in *A. taxiformis* and *G. lanceola* extracts, indicating the presence of sulphated galactose residues in these species. The band at 845 cm^{-1}, corresponding to D-galactose-4-sulphate (G4S), was detected across all extracts and standards, though with variable intensity, reflecting structural diversity in the sulphation pattern of the galactan backbones. Absorptions at 928 and 933 cm^{-1}, together with shoulders at 1070 cm^{-1}, were assigned to 3,6-anhydro-D-galactose (DA). These were particularly prominent in extracts derived from larger Timatic vessels (1-L and 2-L) for *A. taxiformis* and *G. lanceola*, as well as in the direct extract of *N. elminthoides*. This suggests that process scale and extraction intensity may influence the detectable abundance of DA moieties. Broader bands between 1010–1030 cm^{-1} and at 1150 cm^{-1} correspond to C–C and C–O stretching within the pyranoid ring and were present in all extracts, as expected for polysaccharide-rich materials. Finally, absorptions at 1210 and 1260 cm^{-1}, attributed to sulphate esters, were particularly evident in the 1-L *A. taxiformis* extract, the 2-L *G. lanceola* extract, and the direct *N. elminthoides* extract, indicating a relative high degree of sulphation in these samples. Together, these spectral features confirm that the extracted polysaccharides retain structural motifs consistent with sulphated galactans but also highlight species- and process-dependent variation in sulphation pattern and anhydro-galactose content. Such differences are relevant for downstream applications, since biological activities and gelling properties of the standards used are strongly influenced by the type and distribution of sulphate substitutions. On the other hand, the correlation analysis between carrageenan

and κ-carrageenan revealed nearly identical values across all species and extraction conditions. This strong alignment suggests that κ-carrageenan represents the dominant carrageenan type present in the studied red macroalgae. The fact that the values varied only marginally further supports the predominance of κ-carrageenan in the carrageenan fraction, indicating minimal contribution from other carrageenan subtypes. Among the studied species, *G. lanceola* consistently exhibited the highest correlation values, reinforcing its status as a rich source of κ-carrageenan. By contrast, *N. elminthoides* displayed the lowest values, suggesting lower overall carrageenan content or greater structural heterogeneity in its polysaccharide profile. The close correlation between total carrageenan and κ-carrageenan also suggests that targeted extraction of κ-carrageenan could be an efficient strategy for biorefinery processes aimed at maximizing polysaccharide recovery. Agar and agarose standards showed lower correlation with the polysaccharides extracted from the macroalgae. This may be attributed to the predominance of sulfated galactans, typified by carrageenans, in the cell walls of red macroalgae rather than agar (Mendes et al. 2024), suggesting a closer structural and compositional similarity to carrageenan standards.

Principal Component Analysis (PCA)

The PCA provided important insight into species-specific extraction behavior and its implications for the biorefinery strategy. Axis 1 captured the major compositional trade-off between polysaccharide and solid residue quantity, enabling a clear differentiation among the three macroalgae. The vertical dispersion of *N.elminthoides* indicates that its extraction performance is strongly influenced by process scale. Unlike the other species, whose clustering remained tight across control, *N. elminthoides* showed scale-dependent shifts that likely reflect differences in extraction kinetics at larger volumes. Such sensitivity suggests that process optimization for this species may require more refined control of operational parameters. Overall, the PCA highlights that the suitability of each species for specific biorefinery fractions is not only determined by intrinsic biochemical composition but also by how these characteristics interact with extraction scale. *G. lanceola* appears highly robust and predictable, making it a promising candidate for polysaccharide-focused valorization routes. *A. taxiformis* may require more intensive or targeted extraction approaches to overcome its high residual biomass. *N. elminthoides* also demands scale-adjusted processing to maintain yields of bioactive compounds. These findings reinforce the importance of tailoring biorefinery workflows to species-specific properties and to the operational scale at which they are implemented.

Conclusions

The biorefinery approach applied in this study enabled the sequential extraction of multiple valuable compounds, including proteins, bioactive extracts, and polysaccharides, achieving 21% overall biomass utilization efficiency. This study demonstrated the optimization of biorefinery extraction of protein and PE from red macroalgae, highlighting *G. lanceola* as the most promising species of those tested. The highest concentrations of protein and PE were obtained using optimized extraction conditions, including biomass and extraction cycle number, which differed between species. *A. taxiformis* and *N. elminthoides* exhibited different extraction patterns, with *A. taxiformis* showing a greater discrepancy between total protein and PE concentrations. *G. lanceola* demonstrated the highest concentration of extracted soluble protein and polysaccharides, whereas *A. taxiformis* exhibited the highest concentration of bioactive extract. Despite the effectiveness of FPLC in concentrating PE, purity improvements were limited, likely due to size exclusion chromatography constraints. *N. elminthoides* exhibited a promising PE purification potential, reaching a high purity index after FPLC purification, demonstrating its suitability for commercial PE extraction. The analysis of bioactive extracts revealed the presence of hydroxybenzoic and hydroxycinnamic acids, with specific phenolic compounds showing different correlations with extraction scaling. The nitrogen and phosphorus content analysis of the liquid and solid residues derived from the biorefinery suggests that these byproducts could serve as effective biofertilizers. Specifically, the solid residues derived from *A. taxiformis* exhibited significantly higher nitrogen content than those reported in previous studies on red macroalgae, reinforcing their potential for agricultural applications. Similarly, the presence of phosphorus, specifically in the liquid residues of *A. taxiformis* and *N. elminthoides*, further supports their use in sustainable fertilization strategies. Spectroscopic analysis of the extracted polysaccharides confirmed the presence of key structural components. Statistical correlation analysis revealed that the polysaccharides extracted from these macroalgae showed greater structural similarity to carrageenan than to agar standards, reflecting the predominance of sulfated galactans in red seaweed cell walls.

From an applied perspective, these results suggest that extraction workflows can be strategically adapted depending on the intended end-product. Optimizing precipitation strategies, refining chromatographic steps, and integrating scalable equipment could therefore enable efficient, species-specific valorization of red macroalgae biomass in biotechnological and nutraceutical sectors.

Supplementary Information The online version contains supplementary material available at https://doi.org/10.1007/s10811-025-03779-4.

Acknowledgements This work is supported by National Funds by FCT –Portuguese Foundation for Science and Technology, under the projects UID/04033/2025: Centre for the Research and Technology of Agro-Environmental and Biological Sciences and LA/P/0126/2020 (https://doi.org/10.54499/LA/P/0126/2020).

Author contributions All authors whose names appear on the submission made substantial contributions to the conception, acquisition, analysis and interpretation of data. Drafted the work and revised it critically for important intellectual content. Approved the version to be published and agree to be accountable for all aspects of the work in ensuring that questions related to the accuracy or integrity of any part of the work are appropriately investigated and resolved.

Funding Open access funding provided by FCT|FCCN (b-on).

Data availability The data that support the findings of this study are available from the corresponding author upon reasonable request.

Declarations

Competing interests The authors declare no competing interests.

References

Abdool-Ghany AA, Pollier CGL, Oehlert AM, Swart PK, Blare T, Moore K, Solo-Gabriele HM (2023) Assessing quality and beneficial uses of *Sargassum* compost. Waste Manag 171:545–556

Abraham RE, Su P, Puri M, Raston CL, Zhang W (2019) Optimisation of biorefinery production of alginate, fucoidan and laminarin from brown seaweed *Durvillaea potatorum*. Algal Res 38:101389

Alam S, Singh B, Guldhe A, Raghuvanshi S, Sangwan K (2024) Sustainable valorization of macroalgae residual biomass, optimization of pyrolysis parameters and life cycle assessment. Sci Total Environ 919:170797

Apt KE, Collier JL, Grossman AR (1995) Evolution of the phycobiliproteins. J Mol Biol 248:79–96

Baghel RS (2023) Developments in seaweed biorefinery research: a comprehensive review. Chem Eng J 454:140177

Baghel RS, Suthar P, Gajaria TK, Bhattacharya S, Anil A, Reddy CRK (2020) Seaweed biorefinery: a sustainable process for valorising the biomass of brown seaweed. J Clean Prod 263:121359

Baghel RS, Trivedi N, Reddy CRK (2016) A simple process for recovery of a stream of products from marine macroalgal biomass. Bioresour Technol 203:160–165

Beattie SW, Morançais M, Déléris P, Fleurence J, Dumay J (2018) Extraction of phycocyanin and phycoerythrin pigments. In: Charrier B, Wichard T, Reddy CRK (eds) Protocols for Macroalgae Research. CRC Press, Boca Raton, pp 249–266

Bennet A, Bogorad L (1978) Complementary chromatic adaptation in a filamentous blue-green alga. J Cell Biol 58:419–435

Bo T, McWilliams JC, Frieder CA, Davis KA, Chamecki M (2024) Nutrient replenishment by turbulent mixing in suspended macroalgal farms. Geophys Res Lett 51:e2024GL109128

Campbell I, Macleod A, Sahlmann C, Neves L, Funderud J, Øverland M, Hughes AD, Stanley M (2019) The environmental risks associated with the development of seaweed farming in Europe - prioritizing key knowledge gaps. Front Mar Sci 6:107

Carpena M, Garcia-Perez P, Garcia-Oliveira P, Chamorro F, Otero P, Lourenço-Lopes C, Cao H, Simal-Gandara J, Prieto M (2023) Biological properties and potential of compounds extracted from red seaweeds. Phytochem Rev 22:1509–1540

Chevenier A, Jouanneau D, Ficko-Blean E (2023) Carrageenan biosynthesis in red algae: a review. Cell Surf 9:100097

Chew YL, Lim YY, Omar M, Khoo KS (2008) Antioxidant activity of three edible seaweeds from two areas in South East Asia. LWT-Food Sci Technol 41:1067–1072

Cole AJ, Paul NA, de Nys R, Roberts DA (2017) Good for sewage treatment and good for agriculture: algal based compost and biochar. J Environ Manage 200:105–113

Conteratto C, Artuzo FD, Santos OIB, Talamini E (2021) Biorefinery: a comprehensive concept for the sociotechnical transition toward bioeconomy. Renew Sustain Energy Rev 151:111527

Cotas J, Pacheco D, Araujo GS, Valado A, Critchley AT, Pereira L (2021) On the health benefits vs. risks of seaweeds and their constituents: the curious case of the polymer paradigm. Mar Drugs 19:164

Dang B, Ramaraj R, Huynh K, Le M-V, Tomoaki I, Pham T-T, Luan V, Na P, Tran D (2023) Current application of seaweed waste for composting and biochar: a review. Bioresour Technol 375:128830

del Río P, Flórez-Fernández N, Álvarez-Viñas M, Torres M, Romaní A, Domínguez H, Garrote G (2021) Evaluation of sustainable technologies for the processing of *Sargassum Muticum*: cascade biorefinery schemes. Green Chem 23:7001–7015

Elizondo Sada OM, Hiemstra ISA, Chorhirankul N, Eppink M, Wijffels RH, Janssen AEM, Kazbar A (2024) Pressure-driven membrane processes for the recovery and recycling of deep eutectic solvents: a seaweed biorefinery case study. Biotechnol Rep 43:e00849

Errati H, Bencheqroun SK, Aboutayeb R, Abail Z, Lebbar S, Dari K, Hilali L (2022) Assessment of the red seaweed *Gelidium sesquipedale* by-products as an organic fertilizer and soil amendment. Sustainability 14:14217

Feng Y, Lu H, Hu J, Zheng B, Zhang Y (2022) Anti-aging effects of R-phycocyanin from *Porphyra haitanensis* on HUVEC cells and *Drosophila melanogaster*. Mar Drugs 20:468

George R, John J (2023) Phycoerythrin as a potential natural colourant: a mini review. J Food Sci Technol 58:513–519

Gomes-Dias JS, Teixeira-Guedes CI, Teixeira JA, Rocha CMR (2024) Red seaweed biorefinery: the influence of sequential extractions on the functional properties of extracted agars and porphyrans. Int J Biol Macromol 257:128479

Ghosh T, Mishra S (2020) Studies on extraction and stability of C-phycoerythrin from a marine cyanobacterium. Front Sustain Food Syst 4:102

Guo J, Qi M, Chen H, Zhou C, Ruan R, Yan X, Cheng P (2022) Macroalgae-derived multifunctional bioactive substances: the potential applications for food and pharmaceuticals. Foods 11:3455

Holdt SL, Kraan S (2011) Bioactive compounds in seaweed: functional food applications and legislation. J Appl Phycol 23:543–597

Jayawardhana H, Lee HG, Liyanage N, Nagahawatta D, Ryu B, Jeon YJ (2023) Structural characterization and anti-inflammatory potential of sulfated polysaccharides from *Scytosiphon lomentaria*; attenuate inflammatory signaling pathways. J Funct Foods 102:105446

Jasem M, Merai A, Nizam A (2023) Characterization and *in vitro* antibacterial activity of sulfated polysaccharides from freshwater alga *Cladophora crispata*. Access Microbiol 5:acmi000537

Jiang S, Peng X, Wu Z, Cui H, Wei L, Shao G, Liu N, Wei L (2025) Seaweed residue as a low-cost source for producing cellulose nanofibrils with ultraviolet shielding properties. RSC Adv 15:32882–32893

Koyande A, Show P, Guo R, Tang B, Ogino C, Chang J (2019) Bioprocessing of algal bio-refinery: a review on current advances and future perspectives. Bioengineered 10:574–592

Kumar Y, Singhal S, Tarafdar A, Pharande A, Ganesan M, Badgujar PC (2020) Ultrasound assisted extraction of selected edible macroalgae: effect on antioxidant activity and quantitative assessment of polyphenols by liquid chromatography with tandem mass spectrometry (LC-MS/MS). Algal Res 52:102114

Luan C, Lin X, Lin J et al (2024) Integrated biorefinery approach for seaweed *Sargassum fusiforme*: a step towards green circular economy. J Clean Prod 445:141335

Madejón E, Panettieri M, Madejón P, Pérez-de-Mora A (2022) Composting as sustainable managing option for seaweed blooms on recreational beaches. Waste Biomass Valoriz 13:863–875

Martínez-López R, Tuohy M (2023) Rapid and cost-efficient microplate assay for the accurate quantification of total phenolics in seaweeds. Food Chem Mol Sci 6:100166

Martins A, Silva J, Alves C, Pinteus S, Félix C, Augusto A, Pedrosa R, Mestre AS, Santos RMM, Carvalho AP, Goettert M, Laufer S, Lemos MFL (2024) Towards a zero-waste sustainable biorefinery of *Codium* sp. seaweed: from bioactives application to soil enhancement materials. J Clean Prod 453:142191

Mendes M, Cotas J, Pacheco D, Ihle K, Hillinger A, Cascais M, Marques J, Pereira L, Gonçalves A (2024) Red seaweed (Rhodophyta) phycocolloids: a road from the species to the industry application. Mar Drugs 22:432

Mettwally WSA, Gamal AA, Shams El-Din NG, Hamdy AA (2022) Biological activities and structural characterization of sulfated polysaccharide extracted from a newly Mediterranean Sea record *Grateloupia gibbesii* Harvey. Biocatal Agric Biotechnol 45:102487

Mughunth RJ, Velmurugan S, Mohanalakshmi M, Vanitha K (2024) A review of seaweed extract's potential as a biostimulant to enhance growth and mitigate stress in horticulture crops. Sci Hortic 334:113312

Nazemi F, Karimi K, Denayer JFM, Shafiei M (2021) Techno-economic aspects of different process approaches based on brown macroalgae feedstock: a step toward commercialization of seaweed-based biorefineries. Algal Res 58:102366

Nunes N, Valente S, Ferraz S, Barreto MC, de Pinheiro Carvalho MAA (2018) Nutraceutical potential of *Asparagopsis taxiformis* (Delile) Trevisan extracts and assessment of a downstream purification strategy. Heliyon 4:957

Nunes N, Valente S, Ferraz S, Barreto MC, Pinheiro de Carvalho MAA (2019) Constructing ethanol-derived bioactive extracts using the brown seaweed *Zonaria tournefortii* (J.V.Lamouroux) Montagne performed with Timatic extractor by means of response surface methodology (RSM). J Appl Phycol 32:2321–2333

Pacheco D, Matos J, Afonso C, Cardoso C (2025) Application of wet route extraction and its potential for attaining biologically active compounds from seaweed biomass: the case-study of *Gracilaria gracilis*. J Appl Phycol 37:2793–2807

Pereira T, Barroso S, Mendes S, Amaral RA, Dias JR, Baptista T, Saraiva JA, Alves NM, Gil MM (2020) Optimization of phycobiliprotein pigments extraction from red algae *Gracilaria gracilis* for substitution of synthetic food colorants. Food Chem 321:126688

Pillay L, Olasehinde T, Olofinsan K, Erukainure O, Islam S, Olaniran A (2024) Antidiabetic potentials of crude and purified sulphated polysaccharides isolated from *Gracilaria gracilis*, a seaweed from South Africa. Heliyon 10:e35729

Qin L, Xu H, He Y, Liang C, Wang K, Cao J, Qu C, Miao J (2022) Purification, chemical characterization and immunomodulatory activity of a sulfated polysaccharide from marine brown algae *Durvillaea antarctica*. Mar Drugs 20:223

Rajauria G (2018) Optimization and validation of reverse phase HPLC method for qualitative and quantitative assessment of polyphenols in seaweed. J Pharm Biomed Anal 148:230–237

Ruiz-Medina MA, Sansón M, González-Rodríguez ÁM (2022) Changes in antioxidant activity of fresh marine macroalgae from the Canary Islands during air-drying process. Algal Res 66:102798

Romay C, Armesto J, Remirez D, González R, Ledon N, García I (1998) Antioxidant and anti-inflammatory properties of C-phycocyanin from blue-green algae. Inflamm Res 47:36–41

Santos SAO, Félix R, Pais ACS, Rocha SM, Silvestre AJD (2019) The quest for phenolic compounds from macroalgae: a review of extraction and identification methodologies. Biomolecules 9:847

Sekar S, Chandramohan M (2008) Phycobiliproteins as a commodity: trends in applied research, patents and commercialization. J Appl Phycol 20:113–136

Shafie MH, Kamal ML, Zulkiflee FF, Hasan S, Uyup NH, Abdullah S, Hussin NAM, Tan YC, Zafarina Z (2022) Application of carrageenan extract from red seaweed (Rhodophyta) in cosmetic products: a review. J Indian Chem Soc 99:100613

Shih C, Cheng S, Wong C, Kuo Y, Chou T (2009) Antiinflammatory and antihyperalgesic activity of C-phycocyanin. Anesth Analg 108:1303–1310

Sonani RR (2016) Recent advances in production, purification and applications of phycobiliproteins. World J Biol Chem 7:100

Sudhakar MP, Jagatheesan A, Perumal K, Arunkumar K (2015) Methods of phycobiliprotein extraction from *Gracilaria crassa* and its applications in food colourants. Algal Res 8:115–120

Tenci NA, Ammam F, Austen N, Huang WE, Thompson IP (2024) Red seaweed as an abundant, natural methanogenesis inhibitor for industrial biorefinery. J Clean Prod 454:142166

Tesvichian S, Sangtanoo P, Srimongkol P, Saisavoey T, Buakeaw A, Puthong S, Thitiprasert S, Mekboonsonglarp W, Liangsakul J, Sopon A, Prawatborisut M, Reamtong O, Karnchanatat A (2024) Sulfated polysaccharides from *Caulerpa lentillifera*: optimizing the process of extraction, structural characteristics, antioxidant capabilities, and anti-glycation properties. Heliyon 10:e24444

Trung D, Surits V, Zueva A, Cao H, Shevchenko N, Ermakova S, Thinh P (2024) Anticancer activity *in vitro* of sulfated polysaccharides from the brown alga *Spatoglossum vietnamense*. Molecules 29:4982

U.S. Food and Drug Administration (FDA) (2023) 21 CFR §73.530 — *Spirulina* extract. Code of Federal Regulations, Title 21, U.S. Government Publishing Office. https://www.ecfr.gov/current/title-21/section-73.530

Vega J, Álvarez-Gómez F, Güenaga L, Figueroa FL, Gómez-Pinchetti JL (2020) Antioxidant activity of extracts from marine macroalgae, wild-collected and cultivated, in an integrated multi-trophic aquaculture system. Aquaculture 522:735088

Vieira E, Gomes L, Grosso C, Delerue-Matos C (2025) Recent advances on seaweed-derived pigments for food application and current legal framework. Foods 14:3265

Waterborg J (2002) The Lowry method for protein quantitation. In: Walker JM (ed) The Protein Protocols Handbook. Humana Press, Totowa, pp 7–10

Wijesinghe W, Athukorala Y, Jeon YJ (2011) Effect of anticoagulative sulfated polysaccharide purified from enzyme-assistant extract of a brown seaweed *Ecklonia cava* on Wistar rats. Carbohydr Polym 86:917–921

Wirenfeldt CB, Sørensen JS, Kreissig KJ, Hyldig G, Holdt SL, Hansen LT (2022) Post-harvest quality changes and shelf-life

determination of washed and blanched sugar kelp (*Saccharina latissima*). Front Food Sci Technol 2:1030229

Xu Y, Wang Q, Hou Y (2020) Efficient purification of R-phycoerythrin from marine algae (*Porphyra yezoensis*) based on a deep eutectic solvents aqueous two-phase system. Mar Drugs 18:618

Zepeda E, Vásquez-Elizondo RM, Freile-Pelegrín Y, Pliego-Cortés H, Bourgougnon N, Robledo D (2025) Photosynthetic physiology and antioxidant compounds in *Gracilaria cornea* (Rhodophyta) under light modulation. J Appl Phycol 37:1541–1555

Zhao P, Wang X, Niu J, He L, Gu W, Xie X, Wu M, Wang G (2020) Agar extraction and purification of R-phycoerythrin from *Gracilaria tenuistipitata*, and subsequent wastewater treatment by *Ulva prolifera*. Algal Res 47:101862

Zhu X, Healy L, Das RS, Bhavya ML, Karuppusamy S, Sun D-W, O'Donnell C, Tiwari BK (2023) Novel biorefinery process for extraction of laminarin, alginate and protein from brown seaweed using hydrodynamic cavitation. Algal Res 74:103243